# THE SIMULATION AND ANALYSIS OF CARRIER LANDINGS USING A NONLINEAR PILOT MODEL

Clark Albert Wilson

# NAVAL POSTGRADUATE SCHOOL
## Monterey, California

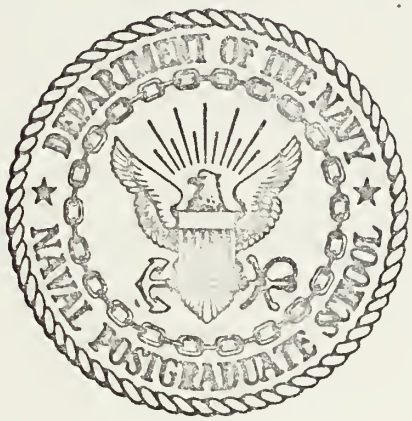


# THESIS

THE SIMULATION AND ANALYSIS OF CARRIER LANDINGS

USING A NONLINEAR PILOT MODEL

by

Clark Albert Wilson

Thesis Advisor: M. H. Redlin

June 1973

# The Simulation and Analysis of Carrier Landings Using a Nonlinear Pilot Model

by

Clark Albert Wilson
Lieutenant, United States Navy
B.S., North Dakota State University, 1965

Submitted in partial fulfillment of the
requirements for the degree of

MASTER OF SCIENCE IN AERONAUTICAL ENGINEERING

from the

NAVAL POSTGRADUATE SCHOOL
June 1973

ABSTRACT

This report investigated the interaction of the pilot and the Fresnel lens optical landing system (FLOLS) with the aircraft system dynamics of a carrier landing and attempted to determine whether or not the dynamics of the FLOLS contributed to a nosedown command by the pilot when approaching touchdown.

With the assumption of a nonlinear pilot model, the entire system's equations of motion were programmed on an analog computer and time histories of approaches for various pilot gains were recorded and analyzed.

Results obtained showed that the stability of the entire system near touchdown was very sensitive to gains which the pilot adopted. Also, because of the lag in the FLOLS dynamics, the pilot would, for some pilot gains, input a definite nosedown command to counteract a rising meatball on the FLOLS display. The typical result of such a command is a hard landing or ramp strike.

TABLE OF CONTENTS

LIST OF TABLES

LIST OF FIGURES

## LIST OF SYMBOLS

$h$ - Perturbation height with respect to glideslope (ft)

$\dot{h}$ - Perturbation height rate with respect to glideslope (ft/sec)

$K_p$ - Pilot gain for p input

M - Pitching moment about C.G.,(ft-lbs)

R - Range from optimum touchdown to aircraft center of mass (ft)

$R_1$ - Range from virtual image to aircraft center of mass (ft)

s - Laplace operator

$T_I$ - Pilot adopted lag time constant (sec)

$T_L$ - Pilot adopted lead time constant (sec)

$T_N$ - Pilot neuromuscular lag time constant (sec)

u - Perturbation velocity in x direction (ft/sec)

$U_c$ - Aircraft speed with respect to aircraft carrier (ft/sec)

$U_o$ - Aircraft speed with respect to air mass (ft/sec)

w - Perturbation velocity in z direction (ft/sec)

X,Z - Components of resultant aerodynamic force acting on airplane (lbs)

$X_m$ - Distance from FLOLS display to virtual image (ft)

z - FLOLS meatball position with respect to datum lights (ft)

$\dot{z}$ - FLOLS meatball velocity with respect to datum lights (ft/sec)

$\delta_e$ - Elevator Position (rad)

$\Delta T$ - Thrust change (lbs)

$\theta$ - Perturbation in pitch (rad)

$\dot{\theta}$ - Perturbation in pitch rate (rad/sec)

$\tau$ - Pilot reaction time (sec)

$(\dot{})$ - $d(\ )/dt$

STABILITY DERIVATIVES

$$X_u^* - \left[\frac{\partial X}{\partial U}\right]_0$$

$$X_w - \left[\frac{\partial X}{\partial W}\right]_0$$

$$Z_u^* - \left[\frac{\partial Z}{\partial U}\right]_0$$

$$Z_w - \left[\frac{\partial Z}{\partial W}\right]_0$$

$$Z_{\dot{w}} - \left[\frac{\partial Z}{\partial \dot{W}}\right]_0$$

$$M_u^* - \left[\frac{\partial M}{\partial U}\right]_0$$

$$M_{\dot{w}} - \left[\frac{\partial M}{\partial \dot{W}}\right]_0$$

$$M_w - \left[\frac{\partial M}{\partial W}\right]_0$$

$$M_q - \left[\frac{\partial M}{\partial q}\right]_0$$

$$X_{\delta_e} - \left[\frac{\partial X}{\partial \delta_e}\right]_0$$

$$Z_{\delta_e} - \left[\frac{\partial Z}{\partial \delta_e}\right]_0$$

$$M_{\delta_e} - \left[\frac{\partial M}{\partial \delta_e}\right]_0$$

$$X_{\Delta T} - \left[\frac{\partial X}{\partial \Delta T}\right]_0$$

$$Z_{\Delta T} - \left[\frac{\partial Z}{\partial \Delta T}\right]_0$$

$$M_{\Delta T} - \left[\frac{\partial M}{\partial \Delta T}\right]_0$$

* Represents Thrust Compensated Derivatives

ACKNOWLEDGEMENTS

The author wishes to express his sincere appreciation to Lieutenant (junior grade) Michael Redlin, Assistant Professor of Aeronautics, for his invaluable guidance, time and assistance during the course of this project, and to Mr. Ralph Smith, Naval Air Development Center, for his suggestions and assistance in the formulation of this study.

# I. INTRODUCTION

The purpose of this report was to simulate and investigate the dynamic interaction of the aircraft, pilot and Fresnel lens optical landing system (FLOLS) during a carrier landing approach. This investigation also sought to determine if the FLOLS dynamics contributed to an increase of sink rate near the ramp.

While attempting to land aboard an aircraft carrier, the pilot receives information from the FLOLS concerning altitude and rate of descent with respect to the glideslope. The allowable deviation from glideslope, when near the ramp, is small and in order to avoid an accident, control of the aircraft must be precise.

The following equation, which describes the $\dot{z}$ motion in the vertical plane of the lens, contains h and $\dot{h}$ terms.

$$\dot{z} = \frac{X_m}{R + X_m} \left[\dot{h} + \frac{U_c h}{R + X_m}\right]$$

Although the aircraft is flown at a constant height above the glideslope, $\dot{z}$ will be positive and the pilot will attempt to control the meatball with elevator. Because $\dot{z}$ lags $\dot{h}$, the pilot may overcontrol and cause an excessive sink rate near the ramp, which can result in an accident or hard landing.

The linear, constant coefficient pilot model derivation in Ref. 1 was not useful for this report because Smith and Reigle [2] reported that this model did not accurately describe how a carrier pilot actually flies. The model shown in Figure 2 was proposed by Smith and Reigle as a better representation of a carrier approach. This model is characterized by nonlinearities in the z and $\dot{z}$ feedback loops. These nonlinear-

ities approximate how the pilot actually flies the approach. Evidence [3] indicated that pilots tended to fly a slightly high meatball and would not make a correction until the ball went slow or exceeded a certain amount on the high side. Additionally, a human pilot is able to discern only a certain amount of movement. The deadspace nonlinearity of the $\dot{z}$ feedback loop represents the pilot's visual perception limit of about 0.2 ft/sec.

In order to validate the model and illuminate reasons for unsatisfactory approaches, an analog computer was programmed for simulation of the equations of motion of the aircraft, pilot model, and FLOLS. The variables of primary interest for this study were the height and height rate deviation from optimum glideslope and the position and rate of motion of the meatball on the FLOLS display as a function of range. The linearized longitudinal equations of motion were used for the aircraft simulation, with the dimensional stability derivatives for the A7E obtained from Ref. [4].

The results expected of this investigation were data which would validate the pilot model, demonstrate a design weakness in the FLOLS and eventually, with further work, provide an operationally reaslistic carrier landing system model which could predict conditions and situations that might result in an accident.

## II. THE FRESNEL LENS OPTICAL LANDING SYSTEM

When the pilot is flying an approach to the carrier, he is primarily controlling his altitude and rate of descent with respect to glideslope ($h$ and $\dot{h}$ respectively). He also controls lateral displacements and rates, but for the purpose of this report these degrees of freedom were ignored. The pilot receives the required information about the aircraft's altitude and rate of descent from the Fresnel lens optical landing system.

The FLOLS consists of five lens cells stacked vertically between two horizontal rows of lights called the datum lights. Each of the five cells consists of three source lamps, a Fresnel lens and a lenticular lens which spreads the beam horizontally to encompass a field of view of 40 degrees. Minimum vertical coverage of the beam is 1.5 degrees for carrier approaches. The lens cells are 10 inches high and are oriented at an angle of 18 minutes to each other. The virtual image, which is 150 feet behind the lens, is an elongated bar of light, but appears as a ball of light until the range is small ($\frac{1}{2}$ second to 1 second before touchdown).

When flying the approach, the pilot attempts to obtain information about $h$ and $\dot{h}$ by interpreting the displacement ($z$) and rate of motion ($\dot{z}$) of the meatball with respect to the datum lights. In order to fly a perfect approach, the meatball must be centered on the datum lights ($z = 0$) and the rate of motion must be zero ($\dot{z} = 0$).

Figure 1 illustrates the geometry of the FLOLS and the various parameters of the lens system. Below, the derivation of the lens equations is shown. All angles were assumed small (i.e., $\theta \approx \tan \theta$).

$$\sigma = \frac{h}{R + X_m} \tag{1}$$

$$z = \sigma X_m$$

$$z = \frac{X_m h}{R + X_m} \tag{2}$$

Next, by taking the derivative of Equation (2) with respect to time:

$$\dot{z} = \frac{X_m}{R + X_m}\left[\dot{h} + \frac{hU_c}{R + X_m}\right] \tag{3}$$

$U_c$ was assumed to be 167 ft/sec for all approaches. By taking the Laplace transform of Equation (3), it can be shown that:

$$\frac{\dot{z}}{\dot{h}}(s) = \frac{X_m}{R + X_m}\left[\frac{s + \frac{U_c}{R + X_m}}{s}\right] \tag{4}$$

For large ranges, $(R + X_m) >> U_c$, Equation (4) becomes:

$$\frac{\dot{z}}{\dot{h}}(s) = \frac{X_m}{R + X_m} \tag{5}$$

Equation (5) demonstrates that for large R and reasonable values of $\dot{h}$, $\dot{z}$ will be below the visual threshold of the pilot, and therefore the $\dot{z}$ feedback loop cannot be active. As the aircraft approaches the carrier $U_c/(R+X_m)$ becomes larger and Equation (4) becomes applicable. Rewriting Equation (4) gives:

$$\frac{\dot{z}}{\dot{h}}(s) = \frac{X_m}{R + X_m} + \frac{U_c X_m}{s(R+X_m)^2} \tag{6}$$

Equation (6) indicates $\dot{z}$ lags $\dot{h}$ because of the second term, which contains an s in the denominator. As the range decreases the lag will become even more pronounced. If the pilot were flying a high ball, the

second term of Equation (3) would provide a $\dot{z}$ indication to the pilot provided $\dot{z}$ were of sufficient magnitude to exceed the visual threshold.

## III. THE PILOT MODEL

Smith and Reigle [2] discussed various pilot models used in the past to describe the method of control that a pilot uses in carrier landings. Most of the models worked well when applied under specified conditions. Durand and Teper [1] suggested a model that was linear and incorporated constant coefficients. This model was valid in two regions, the approach and terminal phase of flight. The model appeared to predict landing statistics fairly well, but Smith and Reigle [2] point out that the approach and terminal model has not been verified for use in predicting ramp strikes, hard landings or in-flight engagements.

Durand and Teper proposed the describing function for a pilot as:

$$Y_p = \frac{K_p e^{-\tau s}(T_N s+1)}{(T_L s+1)(T_I s+1)} \tag{7}$$

During a carrier approach the aircraft motions are essentially low frequency in nature. Therefore, the phugoid closed loop motions, which have a frequency of about 0.2 rad/sec are dominant. The pilot's reaction time, $\tau$, and neuromuscular delay, $T_N$, will contribute only a slight amount and therefore can be neglected. Lag equalization is not useful for carrier approaches and the pilot cannot easily develop effective lead from the information presented by the FLOLS. Therefore, the pilot describing function in the low frequency region can be approximated by pure gains [1].

$$Y_p = K_p \tag{8}$$

Smith and Reigle proposed the system model shown in Figure 2. This model is characterized by multiple feedback loops for control of elevator

and throttle, with nonlinear functions in the z and $\dot{z}$ feedback loops. Also, the model incorporates pure gains as the pilot describing function used for the simulation. The nonlinear functions are unique to pilot modeling and describe more closely how the pilot actually flies an approach. The pilot, in sensing velocity can only perceive motion after it has exceeded his visual perception threshold. The threshold was assumed to be 0.2 ft/sec for this investigation. This means that the pilot cannot close the $\dot{z}$ feedback loop unless $\dot{z}$ exceeds the absolute value of 0.2 ft/sec. The effect of this threshold nonlinearity is to destabilize the system.

Evidence presented by Smith and Reigle [3] indicates that pilots tended to fly the approach so that z was slightly positive. This indifference threshold is shown in the z feedback of Figure 2. The features of the function were that when the aircraft was low with respect to the glideslope, z would have to exceed one foot before the z feedback loop would close.

Since h and $\dot{h}$ cannot accurately be determined by the pilot during a carrier approach, the pilot controls the aircraft by sensing z and $\dot{z}$. In the longitudinal mode, control of the aircraft was achieved by use of elevator and throttle. In this report it was assumed that z would control the throttle and the elevator would be controlled by $\dot{z}$. When near the ramp, throttle response is too slow to control $\dot{z}$, but does not pose any problem in the control of z. Evidence indicates that most pilots fly carrier approaches in this manner [3]. It has been this author's experience (340 carrier landings) that controlling $\dot{z}$ with elevator and z with throttle, close to the ramp, is the safest method.

The pilot usually has, during a daytime approach, good aircraft

attitude clues, such as the horizon. This implies that the pilot has adopted a fairly high gain on $\theta$. However, the gain will not be large enough to make the $\theta$ or $\dot{\theta}$ excursions excessive during the approach. If visual clues deteriorate, or if the pilot is preoccupied with something else, or if he has vertigo, the $\theta$ gain decreases to a point where the system may become destabilized. A dark, moonless night, where there is little horizon, would be an example where the pilot has very little loop closure on $\theta$.

The gain $K_{\dot{z}}$ that the pilot adopts has a range of values dependent upon factors internal and external to the pilot. If the pilot had vertigo, he would have problems trying to close the $\dot{z}$ loop and to some extent, the z loop. In attempting to close the $\dot{z}$ loop, he would probably adopt a high gain to compensate for the lag induced by the vertigo. Another reason for adopting a high gain would be deck-spotting. Many pilots look away from the FLOLS display to the deck for an instant while approaching the ramp. Upon returning the FLOLS the meatball has already acquired a $\dot{z}$ and the pilot, in attempting to stop $\dot{z}$, adopts a high gain.

During a carrier approach, the pilot controls z with power. The importance of $K_z$ can be appreciated when it is realized that varying $K_z$ changes the phugoid damping of the system. An increase of $K_z$ decreases the phugoid damping. This allows the aircraft to respond quicker to error signals in the z feedback loop. Also, the aircraft overshoots and is less stable than if smaller gain values were used.

## IV. RESULTS

The simulation of the system was solved on the analog computer and time histories of various pilot gains are depicted in Figures 3 through 11. The starting point of 20 feet below the glideslope at 2556 feet range from touchdown was used because this is one of the most difficult maneuvers for the pilot to perform and still be able to land safely. One approach starting at 20 feet above the glideslope is shown in Figure 3.

It was found that the outcome of the approach was very sensitive to the gain adopted by the pilot. $K_\theta$, which can be correlated to the quality of the visible horizon, was the most sensitive of the three gains. $K_z$, which controlled the power, was nearly as sensitive as $K_\theta$. When the aircraft was slightly high and the z feedback loop was not active, there were no power changes being applied.

In general, values of $K_\theta$ in the region of 1.75 to 2.5 rad/rad and a fairly low values of $K_z$ (i.e., in the region of 0.003 rad/ft) resulted in a smooth approach with $\dot{h}$ and h not too excessive. Increasing $K_z$ caused the amplitude of $\dot{h}$ and h to increase throughout the approach. $K_{\dot{z}}$ became important whenever the threshold was exceeded, which occurred most of the time near the ramp. The higher gains of $K_{\dot{z}}$ resulted in less variation in $\dot{h}$.

$\dot{z}$ lagged $\dot{h}$ in all approaches and, as a consequence, the control input to the elevator was lagged, which resulted in proper control being late in application. There was a definite nosedown input by the pilot due to the rising meatball close to touchdown.

The z feedback loop nonlinearity was taken out of the loop and

results were similar to results obtained with the nonlinearity in the loop, except the system destabilized at higher $K_\theta$ and $K_z$ than before.

## V. CONCLUSION

As a result of observing the solution of the system for various pilot gains and time histories of the approaches, the following conclusions have been reached:

1. The system model represents an actual carrier approach, except in the case where the model pilot decreased power near the ramp. The reason for the power reduction was because the pilot observed a positive z, greater than the indifference threshold, which call for a decrease in power. However, there was a negative $\dot{z}$ at the same time which demands a nose up command. Thus the aircraft would be put on the backside of the power curve and $\dot{h}$ would actually increase.

2. The system model demonstrates that the FLOLS dynamics can cause the pilot to input a nose down command to the elevators, which increases the sink rate, in response to a positive $\dot{z}$ as perceived when close to the ramp. This result was greatest when $K_\theta$ and $K_{\dot{z}}$ were small, which implies poor visible horizon and not very tight control in the $\dot{z}$ feedback loop. Also this response occurs because $\dot{z}$ lags $\dot{h}$.

3. More research should be undertaken to fully explore the dynamics of the carrier approach using this model. A stability analysis should be performed to determine the zero-pole structure as a function of range.

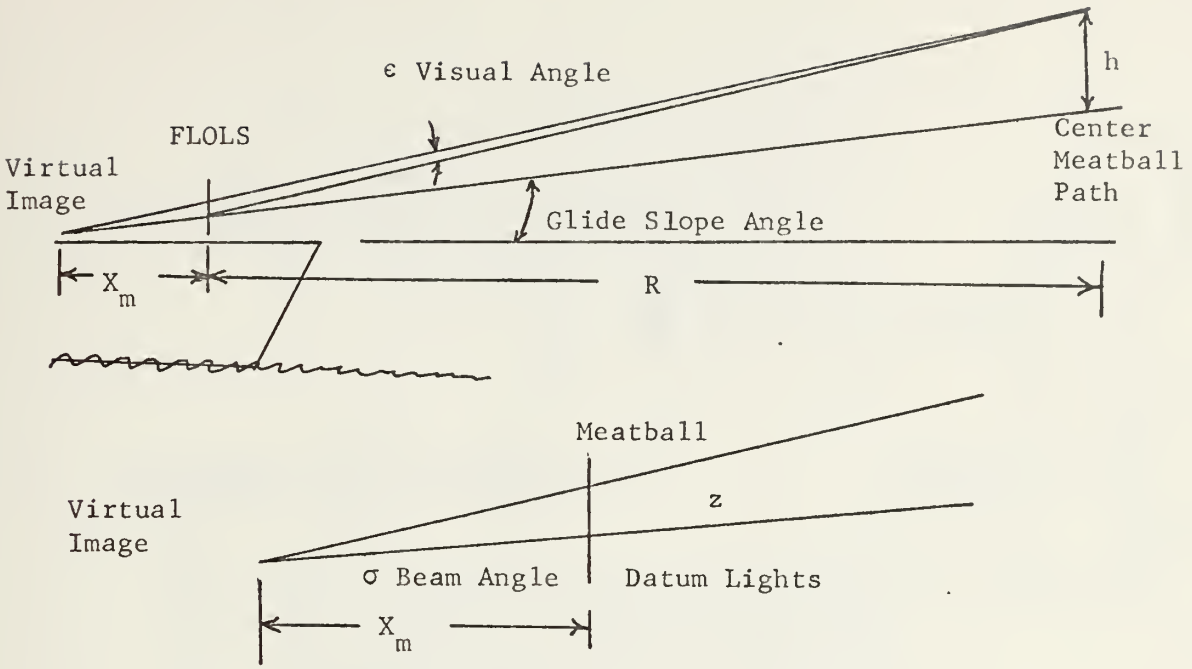


Figure 1. FLOLS Geometry

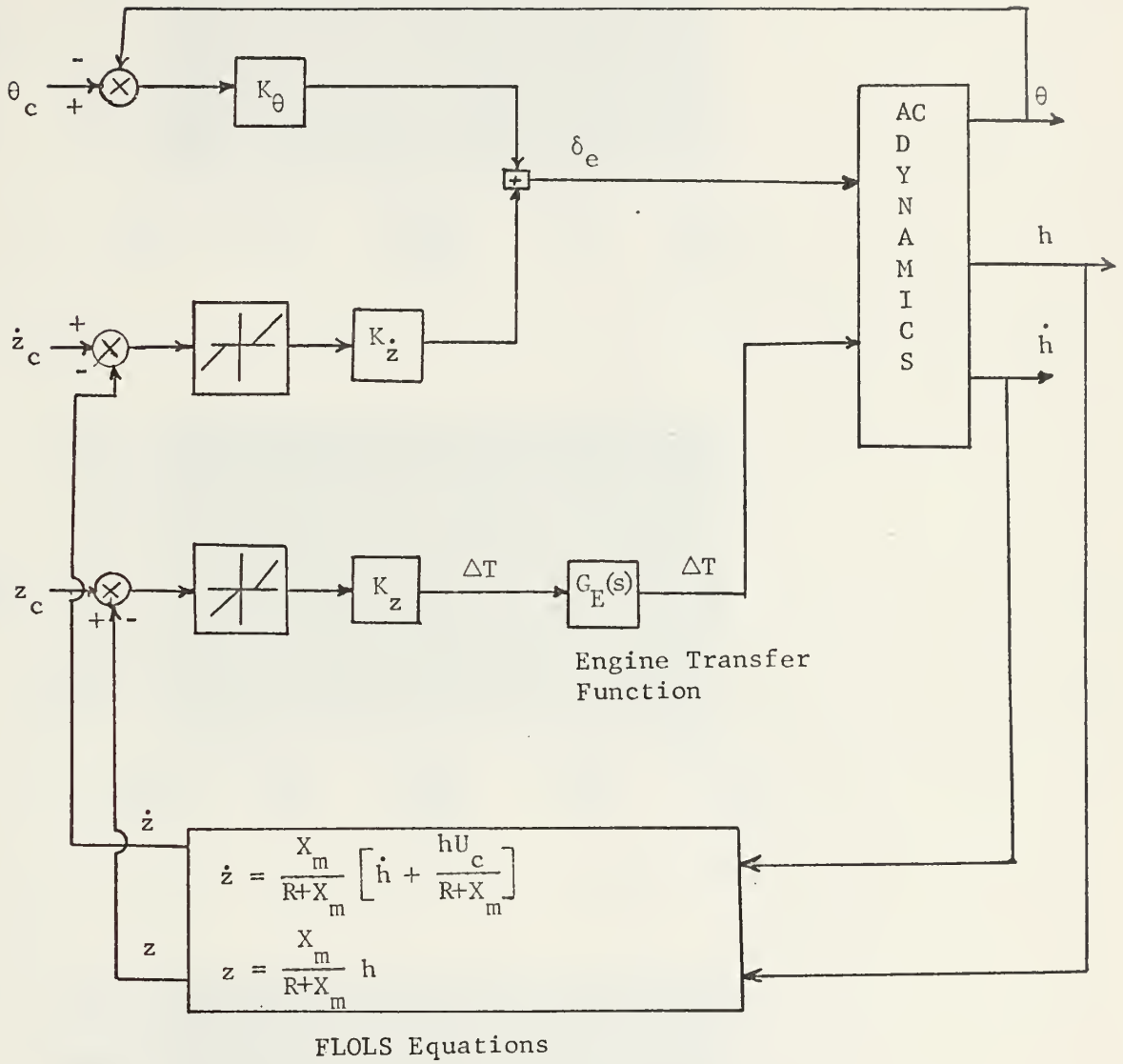


Figure 2. System Diagram for Carrier Approach

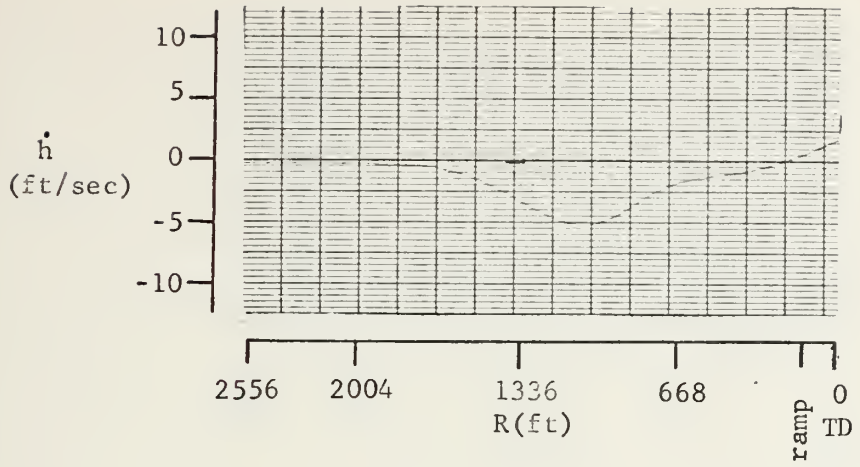


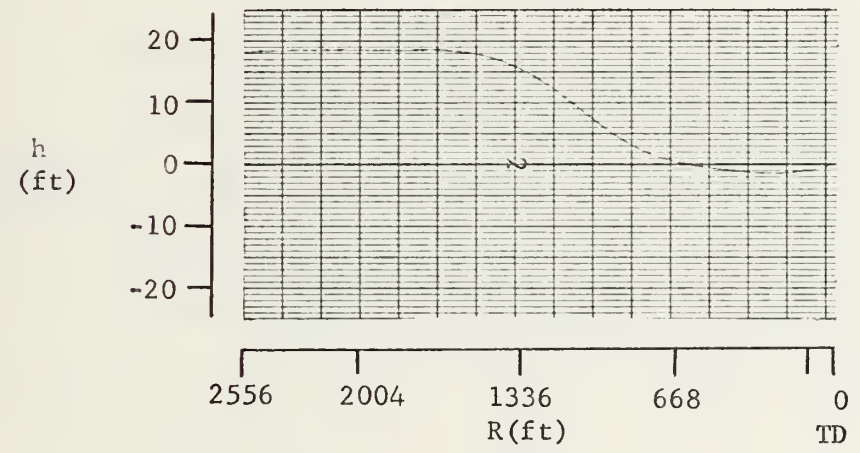


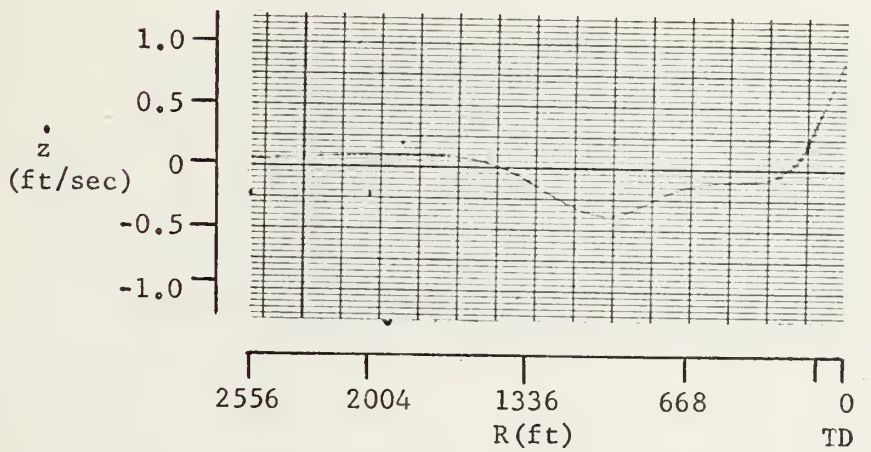


Figure 3. Approach recordings for $K_\theta$ = -1.47 rad/rad, $K_z$ = 0.0524 rad/ft, $K_{\dot{z}}$ = -0.096 rad/ft/sec. Initial condition: h = +20 ft, z = +0.974 ft.

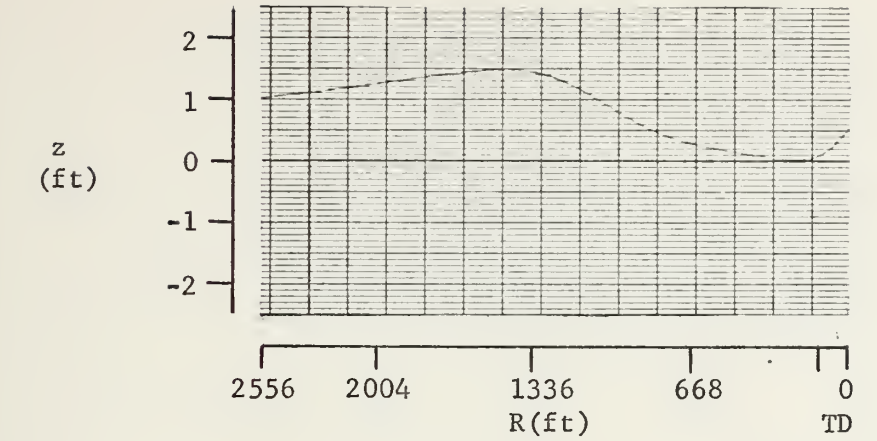


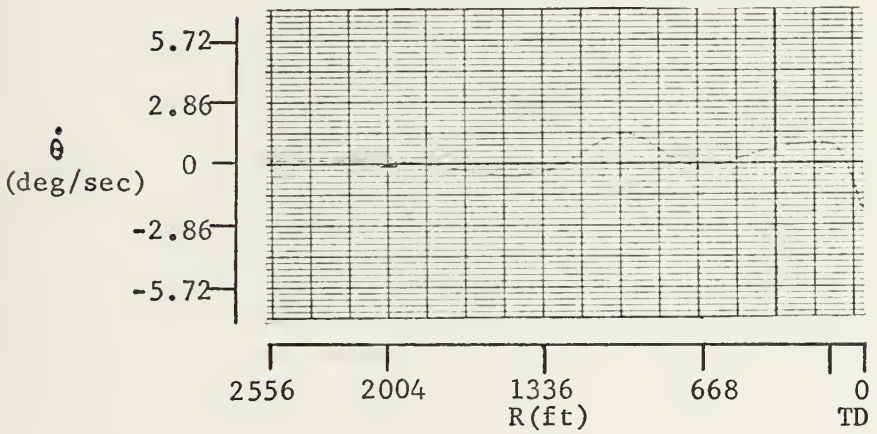


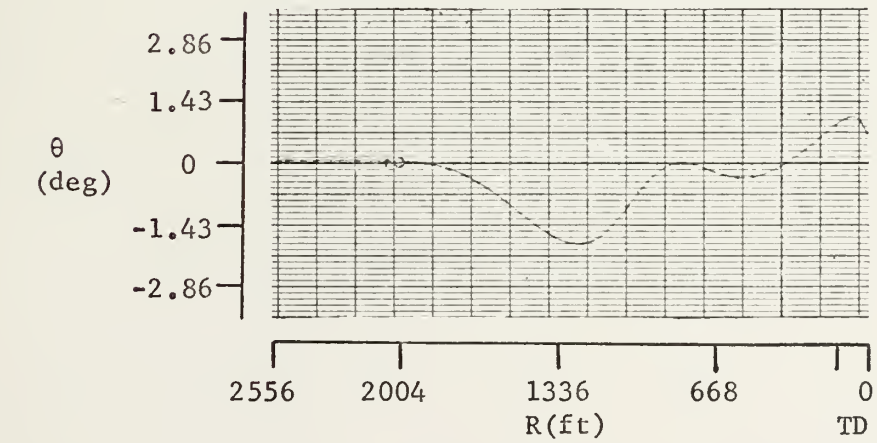


Figure 3 (continued)

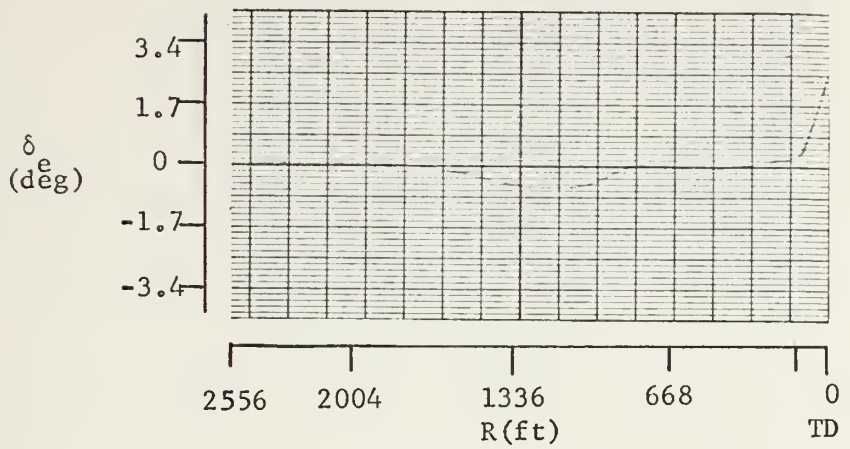


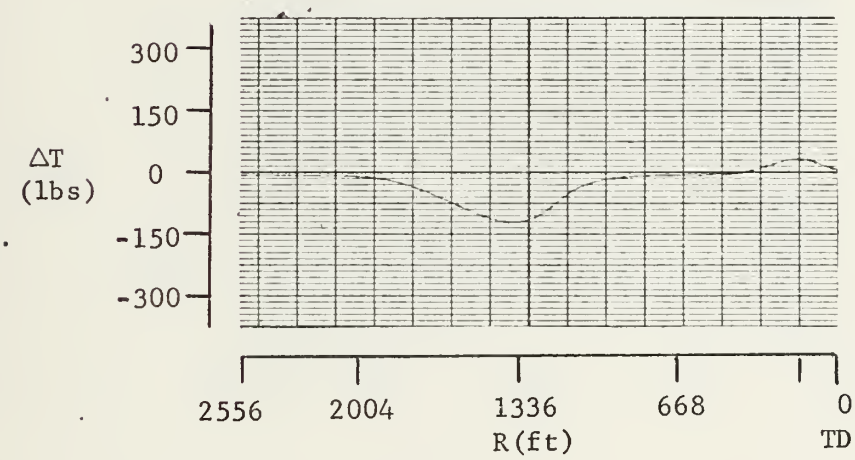


Figure 3 (continued)

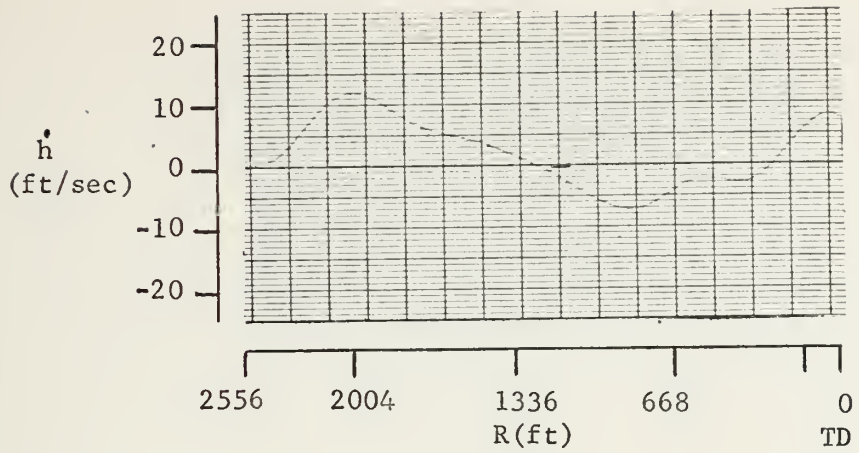


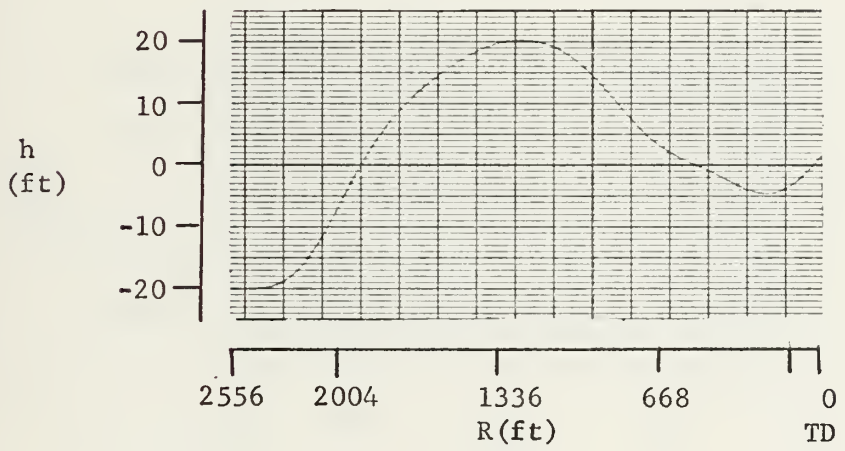


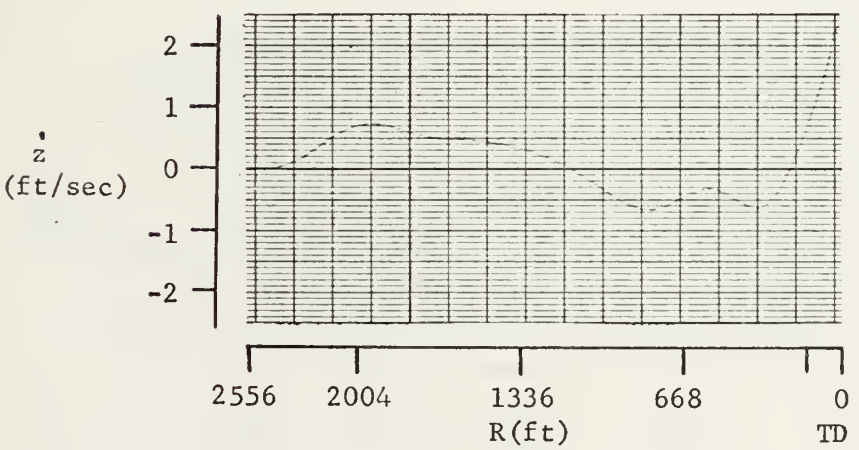


Figure 4. Approach recording for $K_\theta$ = -1.47 rad/rad, $K_z$ = 0.0524 rad/ft, $K_{\dot{z}}$ = -0.096 rad/ft/sec. Initial condition: $^{z}h$ = -20 ft, $z^{z}$ = -0.974 ft.

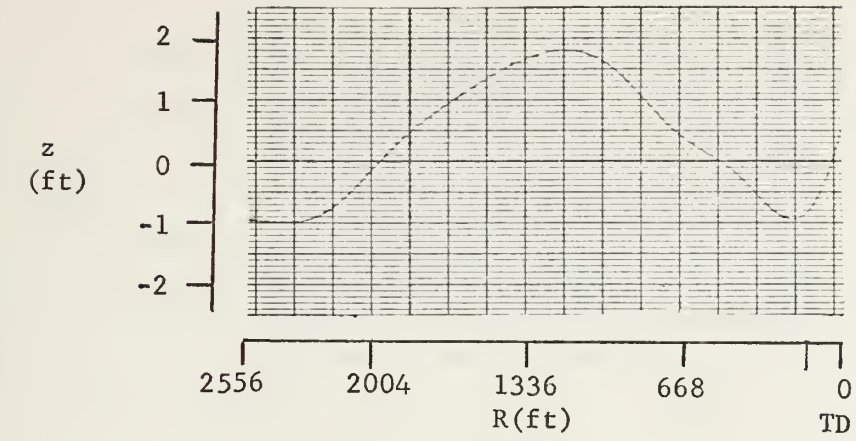


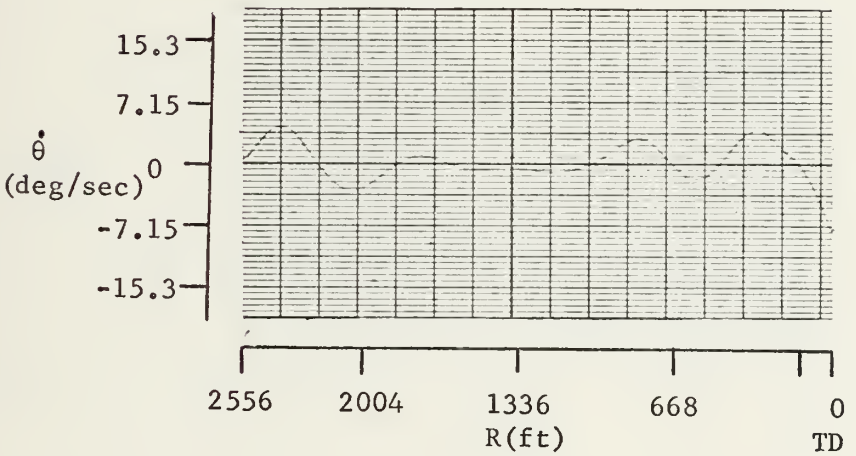


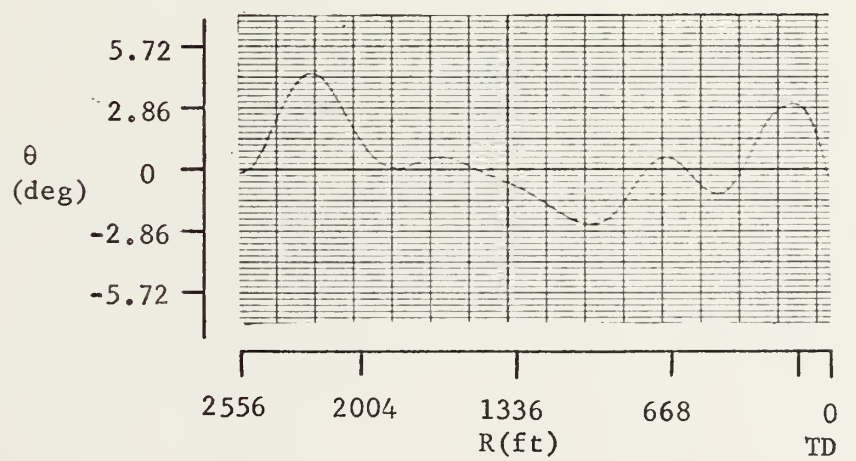


Figure 4(continued)

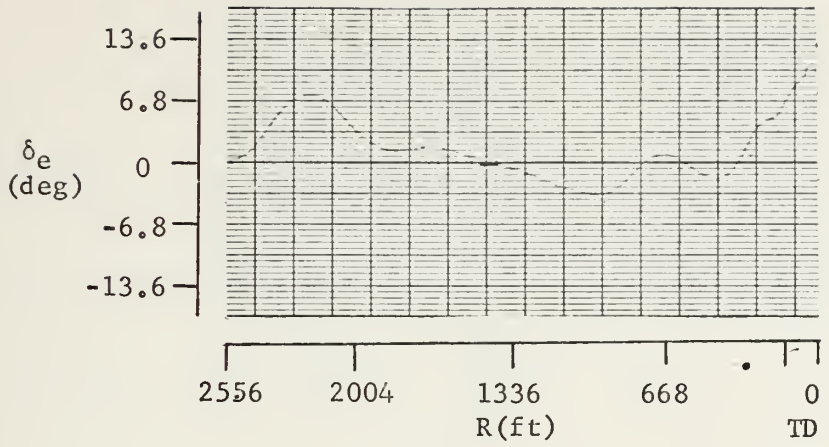


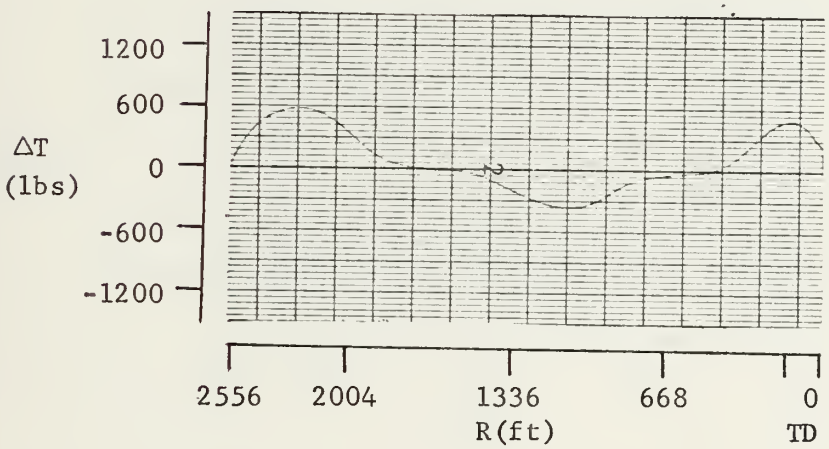


Figure 4 (continued)

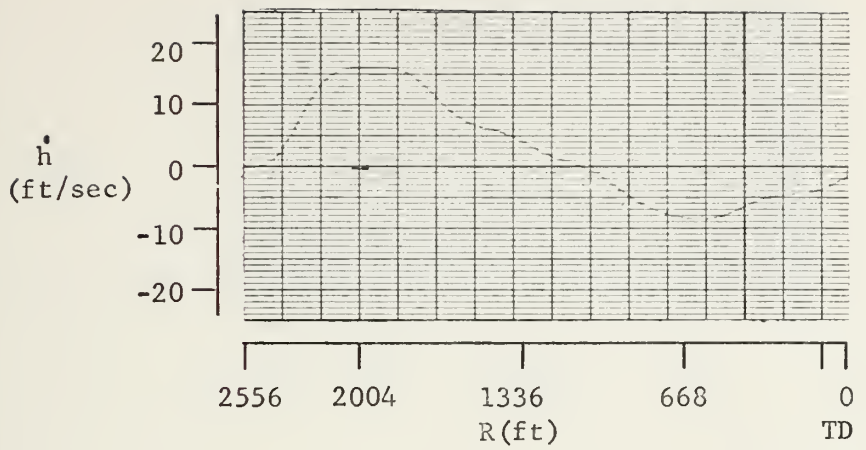


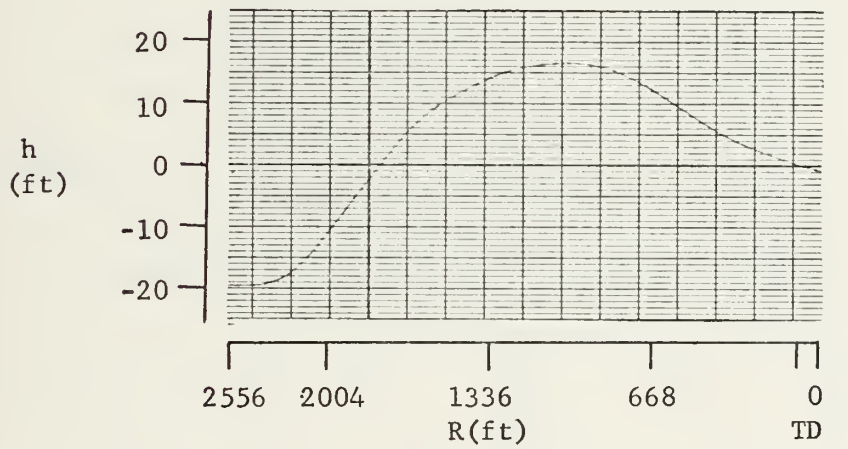


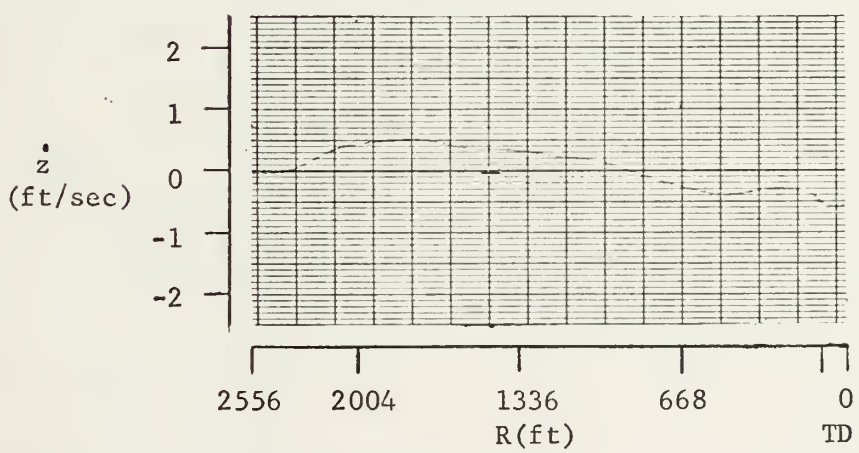


Figure 5. Approach recordings for $K_\theta$ = -2.5 rad/rad, $K_z$ = 0.0524 rad/ft, $K_{\dot{z}}$ = -0.096 rad/ft/sec. Initial conditions: h = -20 ft, $z_z$ = -0.974 ft.

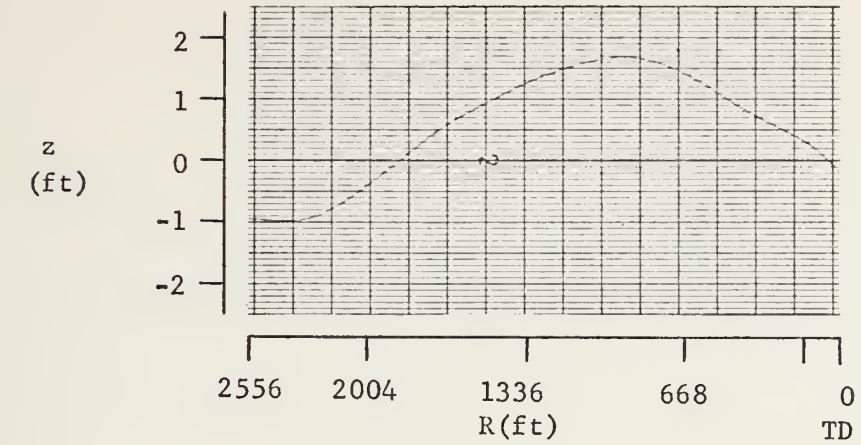


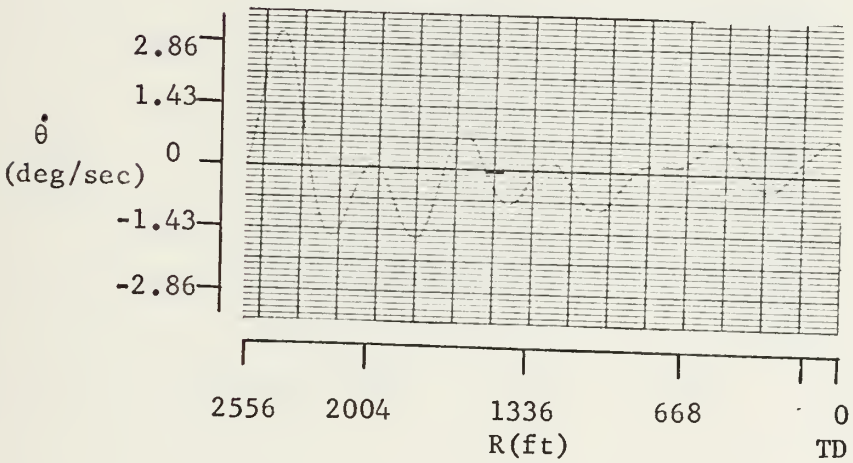


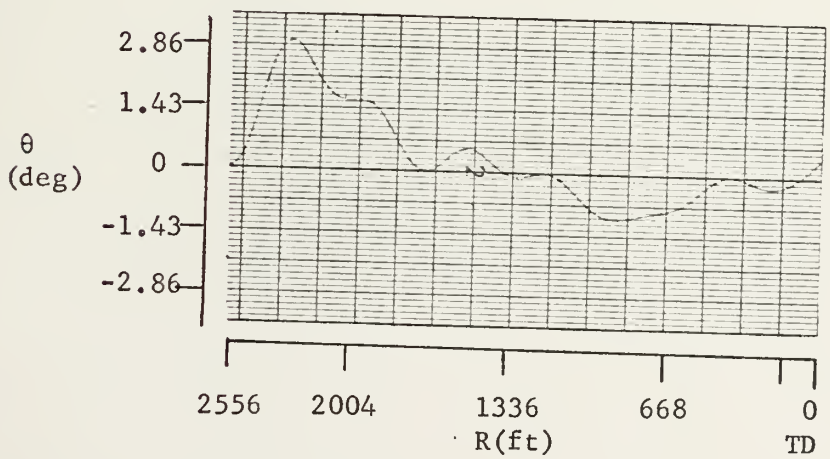


Figure 5 (continued)

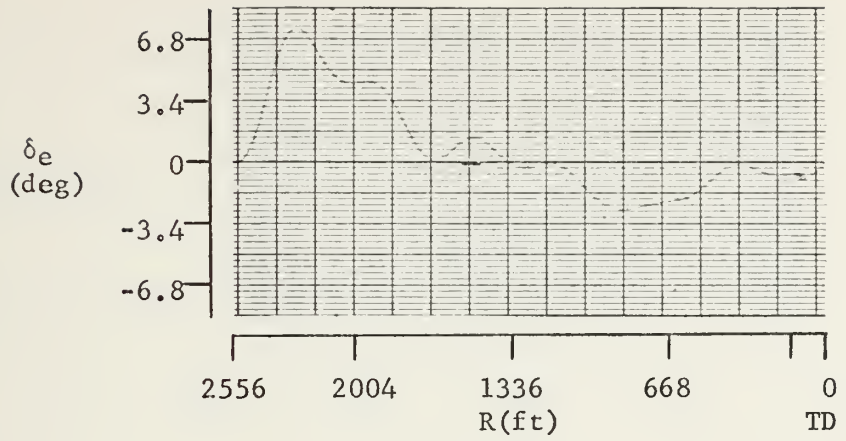


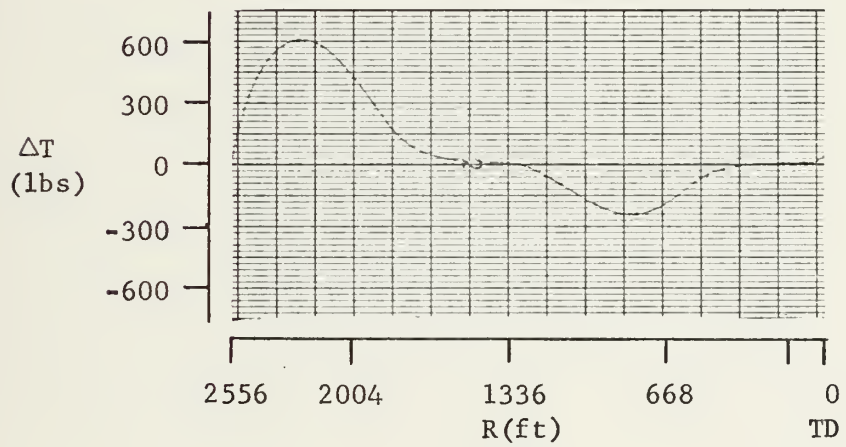


Figure 5 (continued)

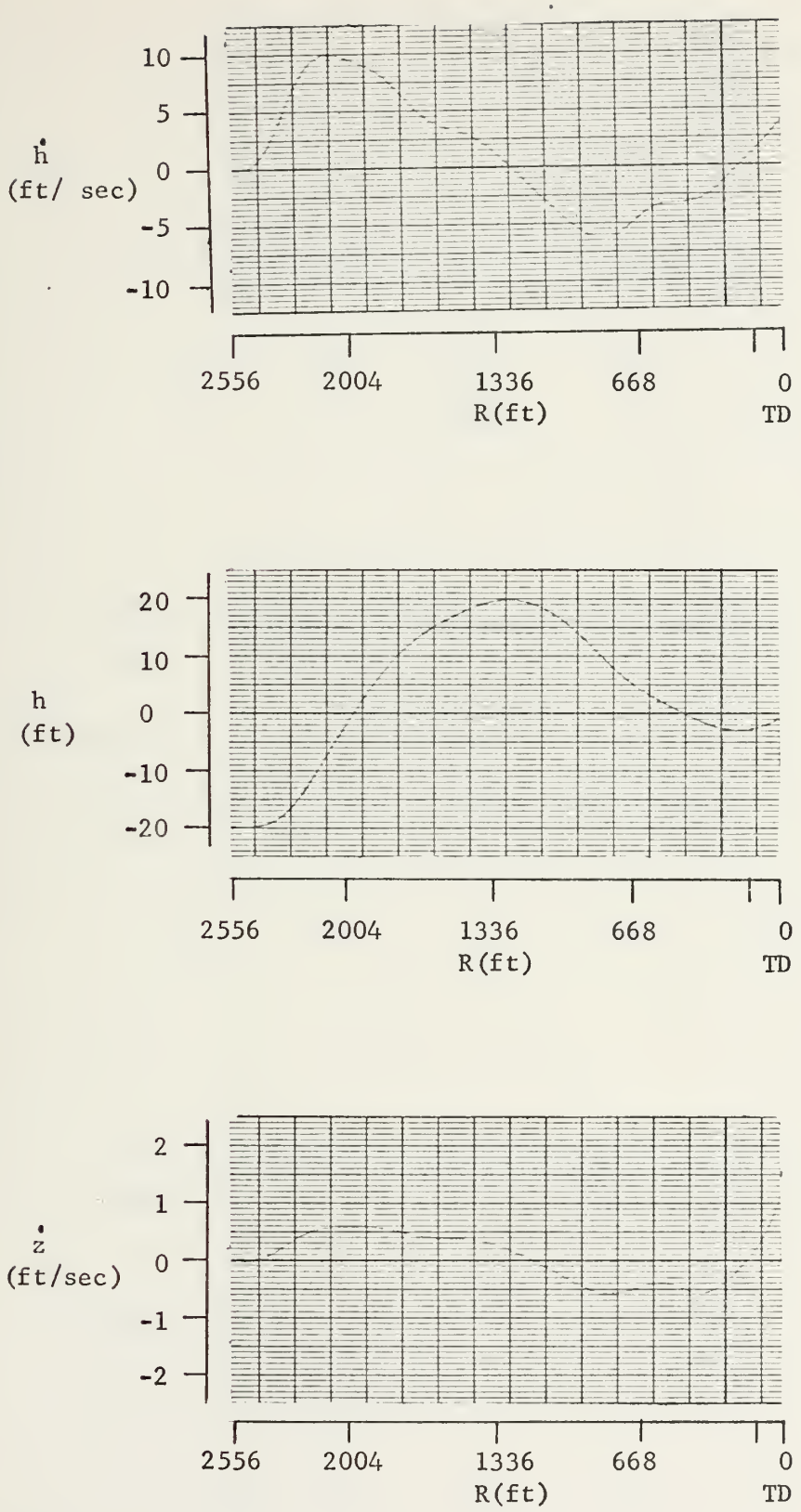


Figure 6. Approach recording for $K_\theta$ = -2.5 rad/rad, $K_z$ = 0.0665 rad/ft, $K_{\dot{z}}$ = -0.096 rad/ft/sec. Initial conditions: h = -20ft, $z^z$ = -0.974 ft.

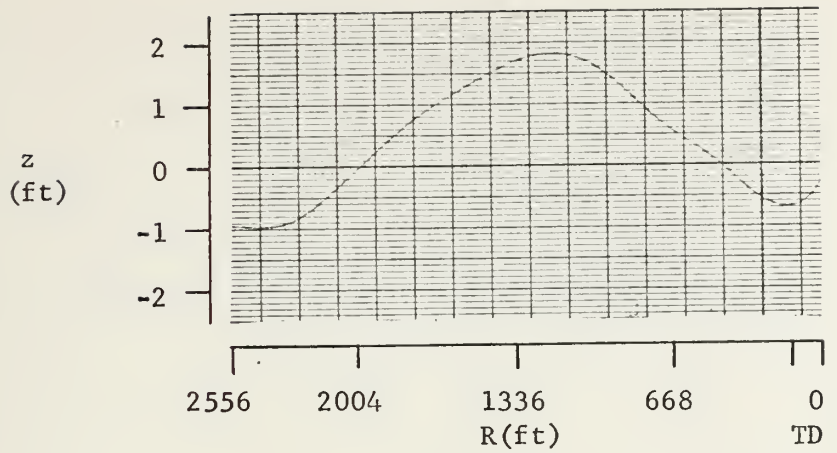


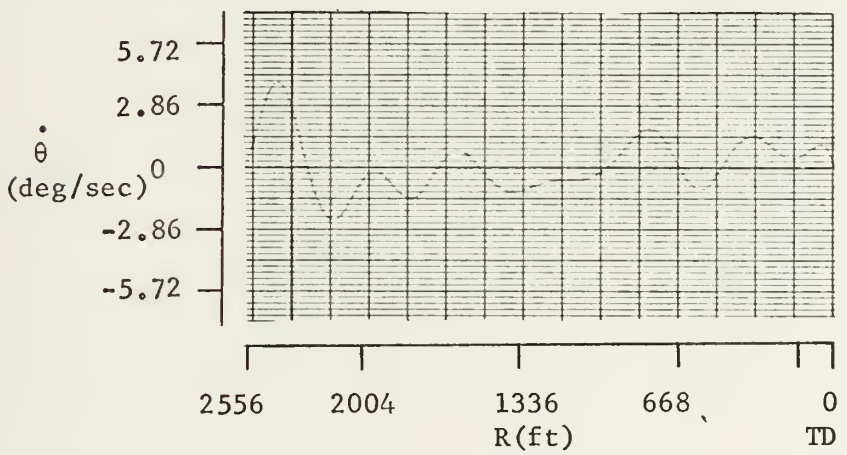


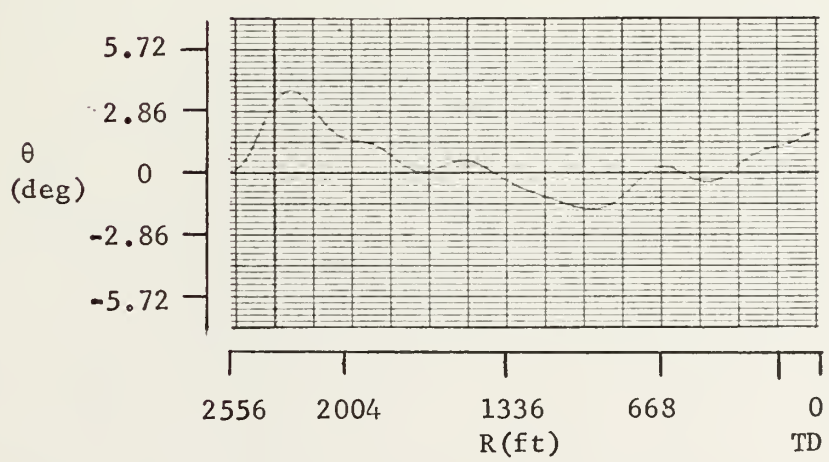


Figure 6 (continued)

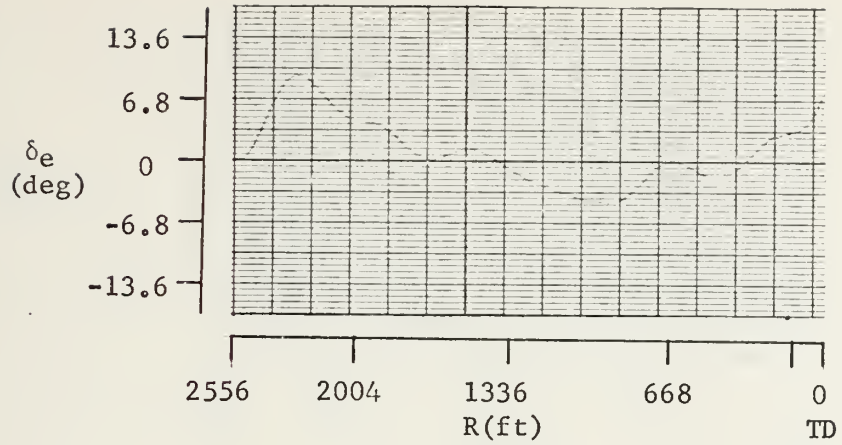


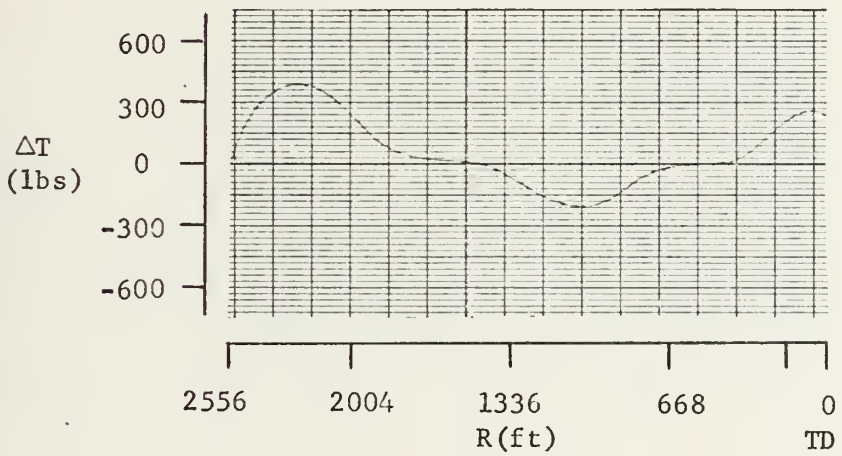


Figure 6 (continued)

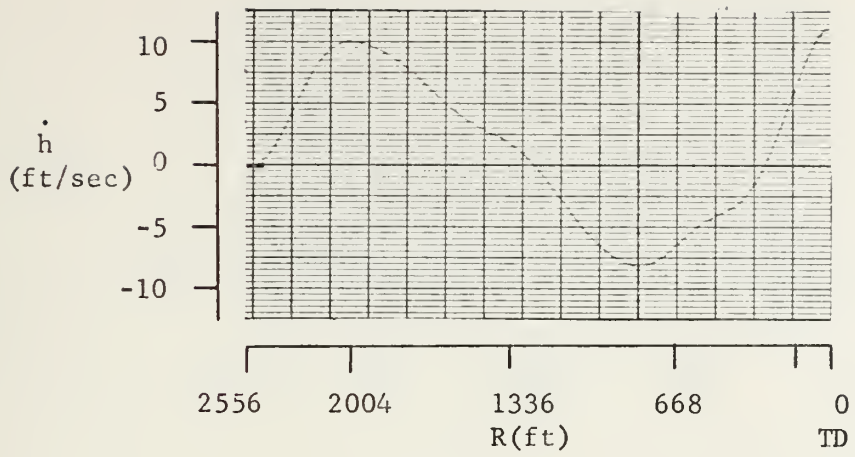


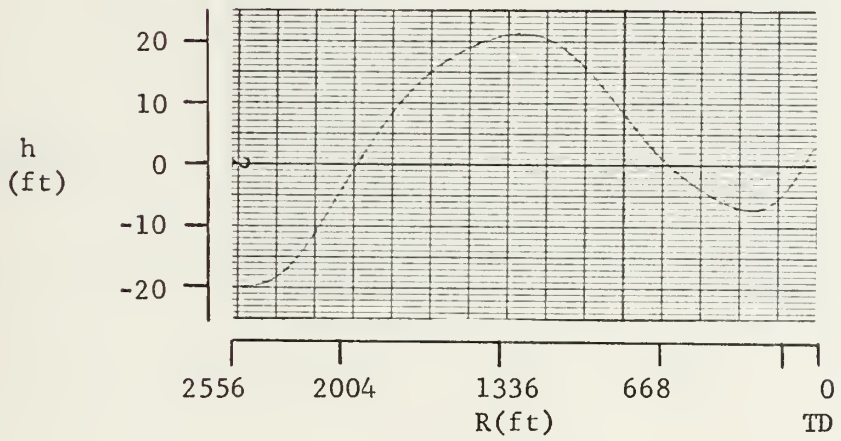


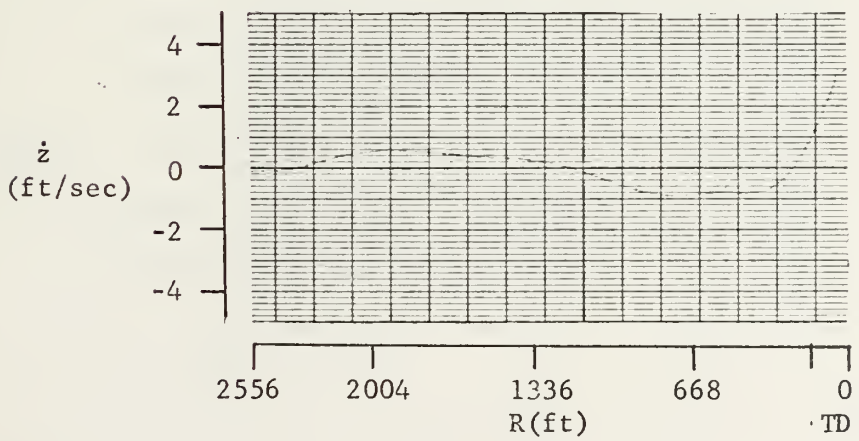


Figure 7. Approach recording for $K_\theta$=-1.75 rad/rad, $K_z$ = 0.0506 rad/ft, $K_{\dot{z}}$=-0.0326 rad/ft/sec. Initial Conditions: h=-20ft,z=-0.974ft.

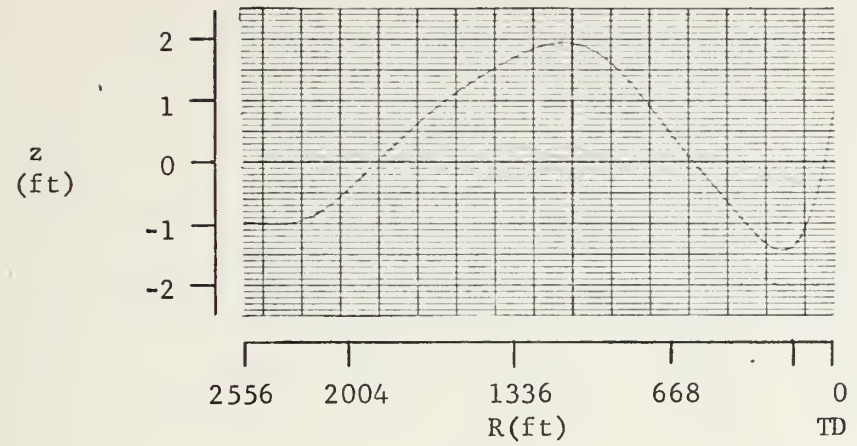


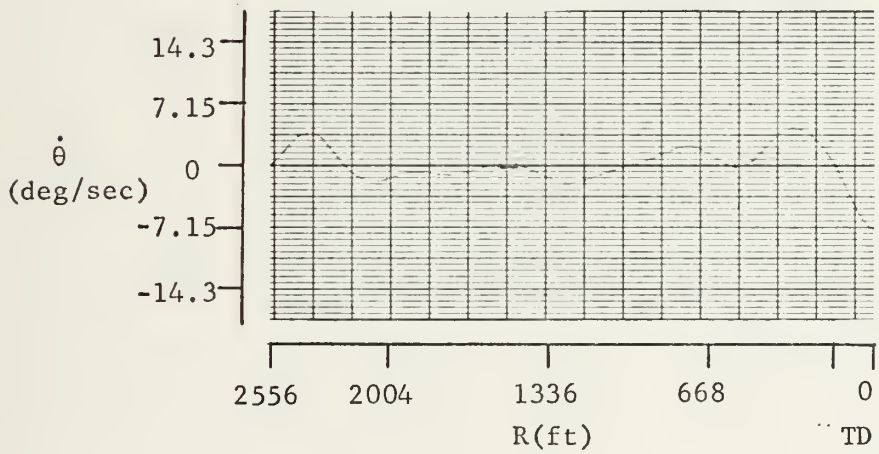


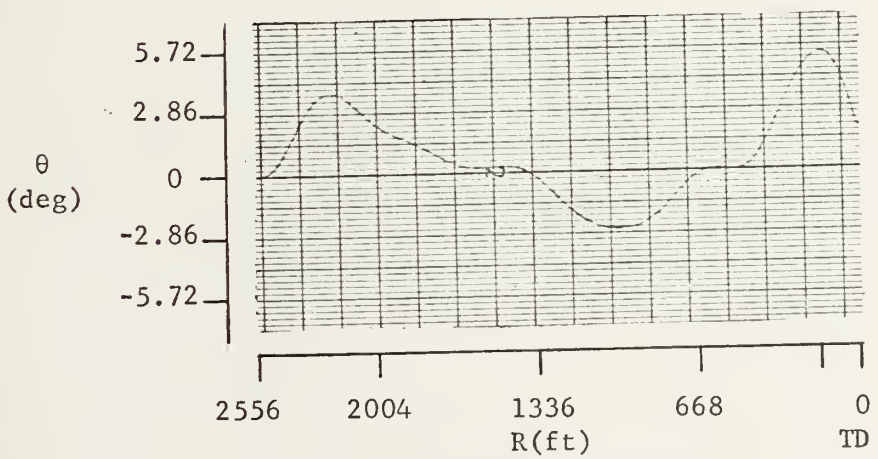


Figure 7 (continued)

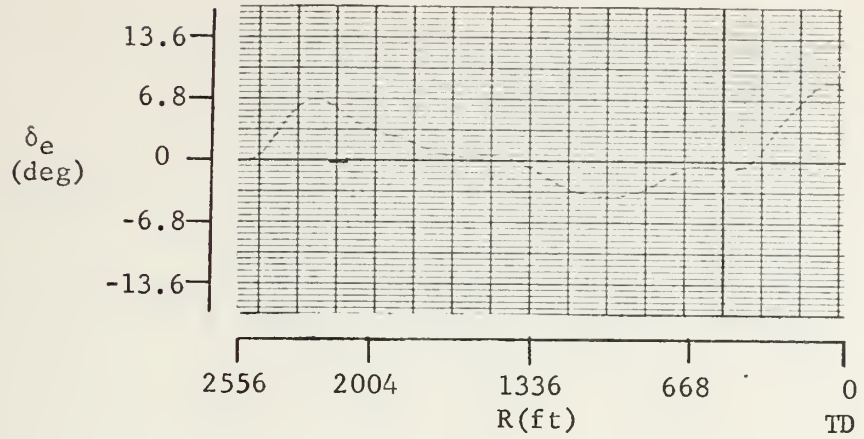


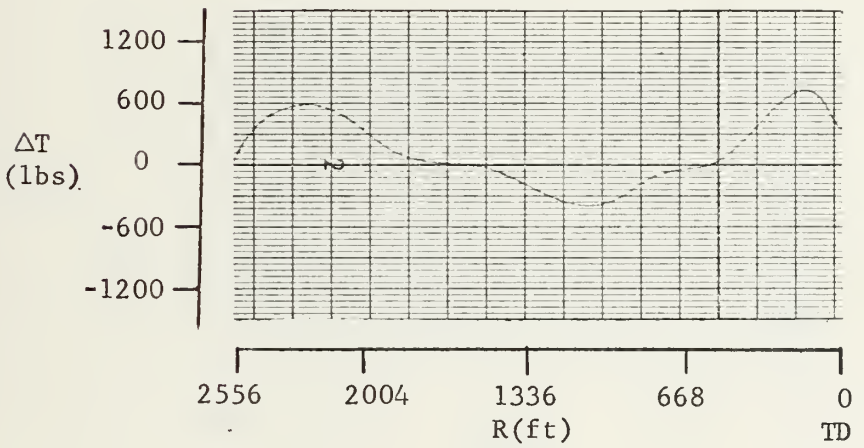


Figure 7 (continued)

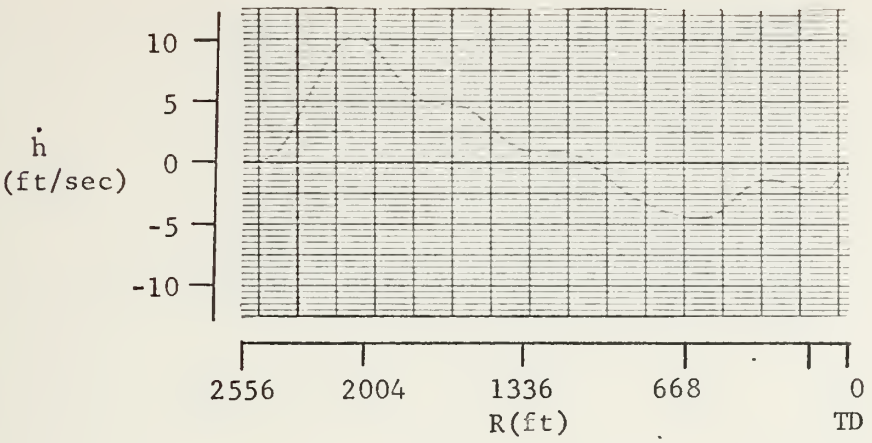


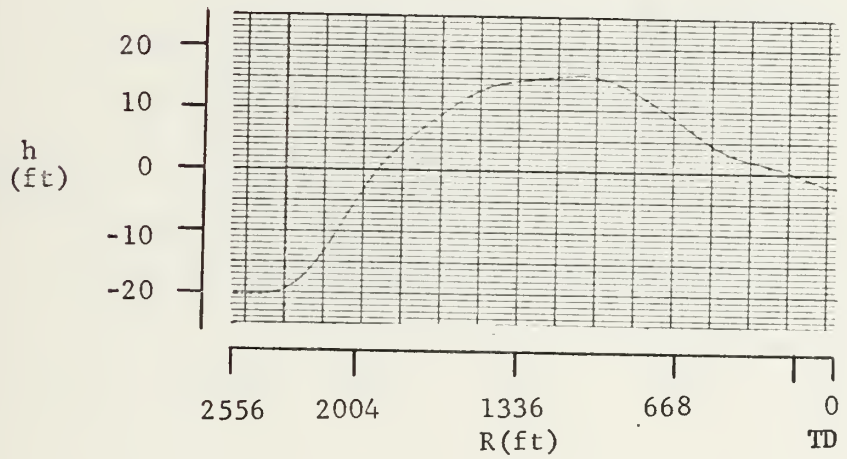


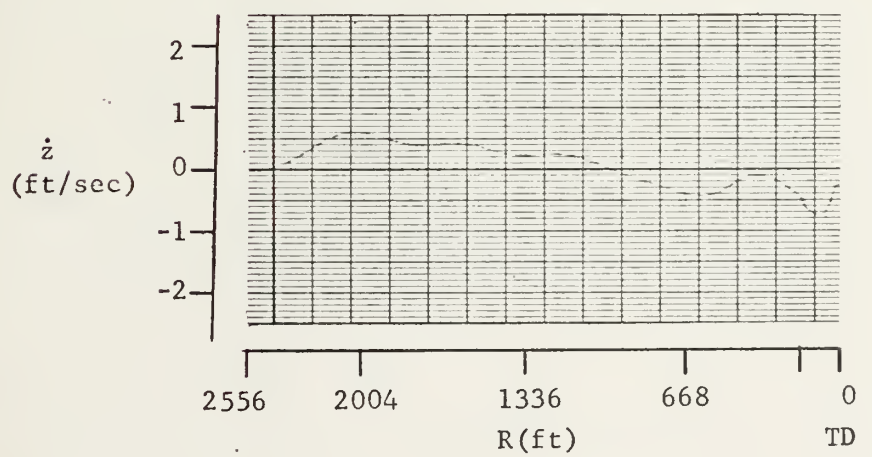


Figure 8. Approach recordings for $K_\theta$=-1.75 rad/rad, $K_z$=0.0506 rad/ft, $K_{\dot{z}}$=-0.318 rad/ft/sec. Initial Conditions: h=-20ft, z=-0.974ft.

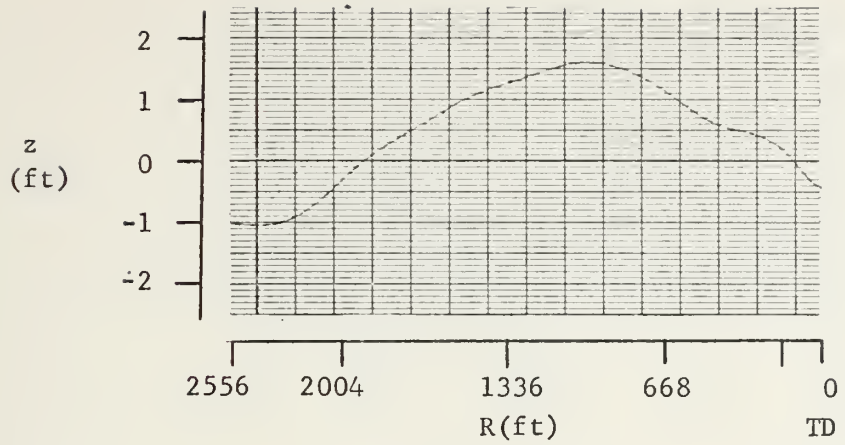


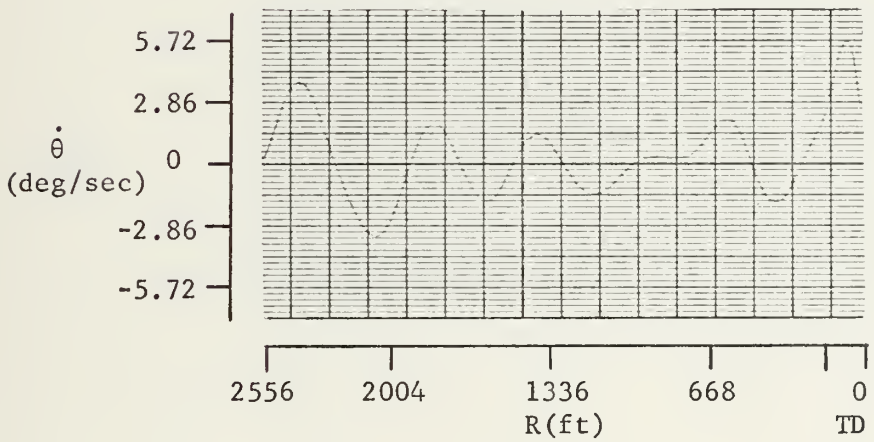


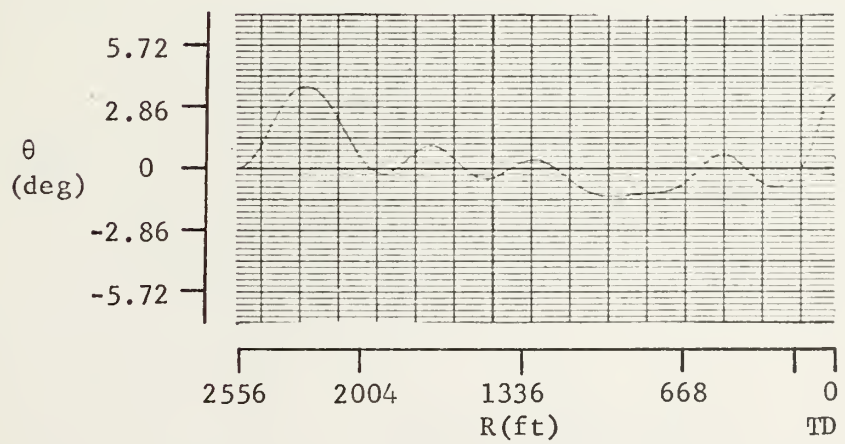


Figure 8 (continued)

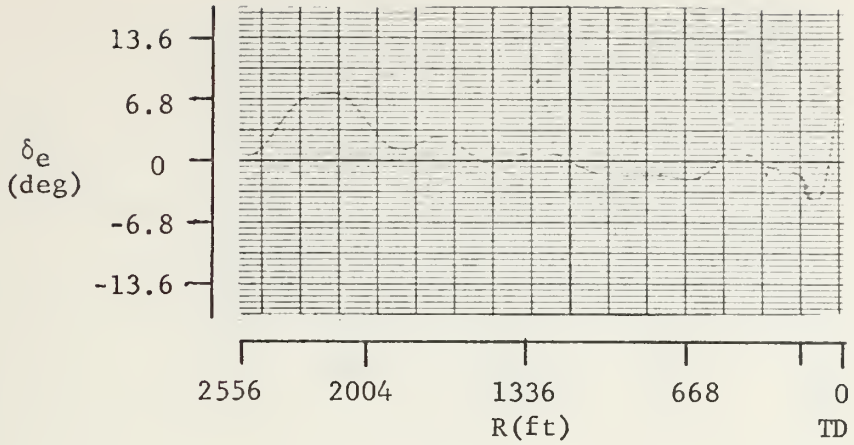


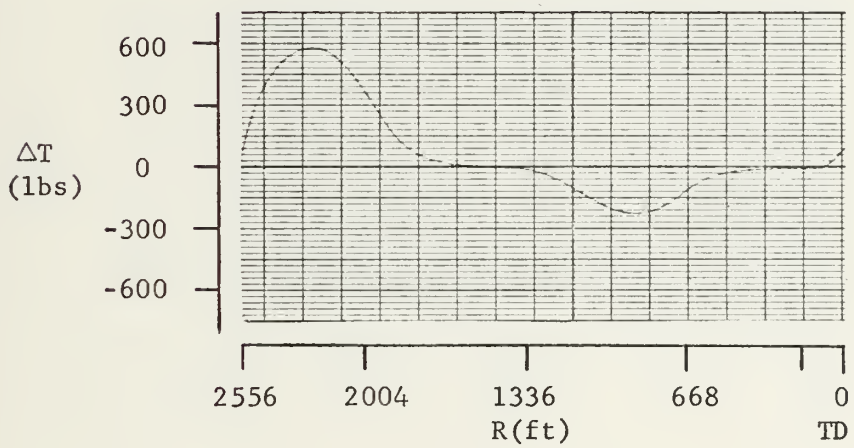


Figure 8 (continued)

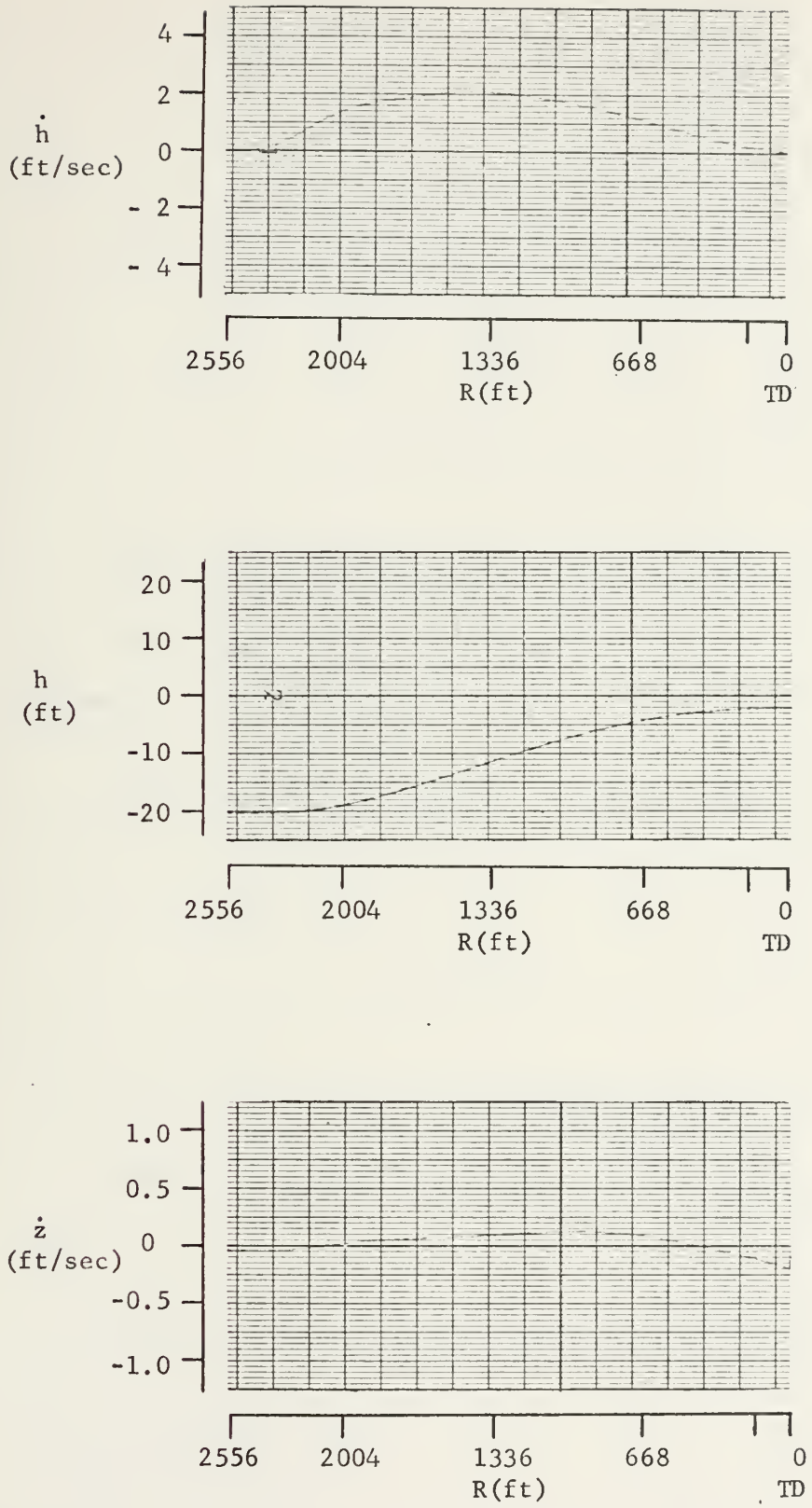


Figure 9. Approach recordings for $K_\theta$=-0.567 rad/rad, $K_z$=0.00342 rad/ft, $K_{\dot{z}}$=-0.201 rad/ft/sec. Initial Condition: h=-20ft, z=0.974ft.

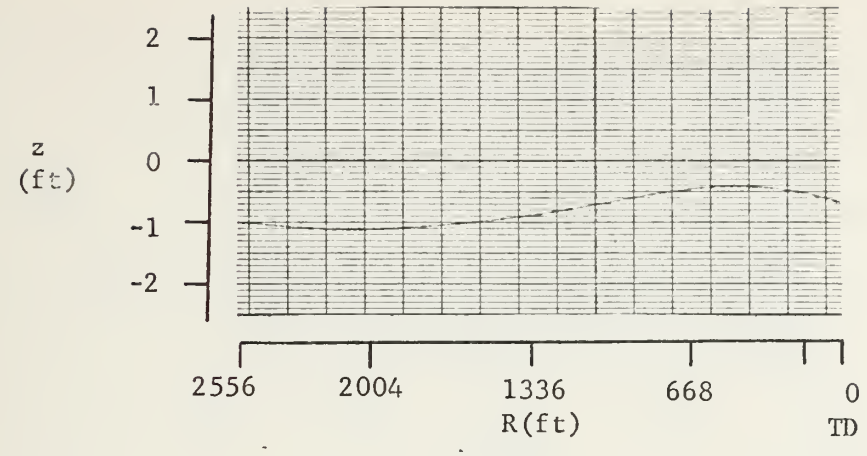


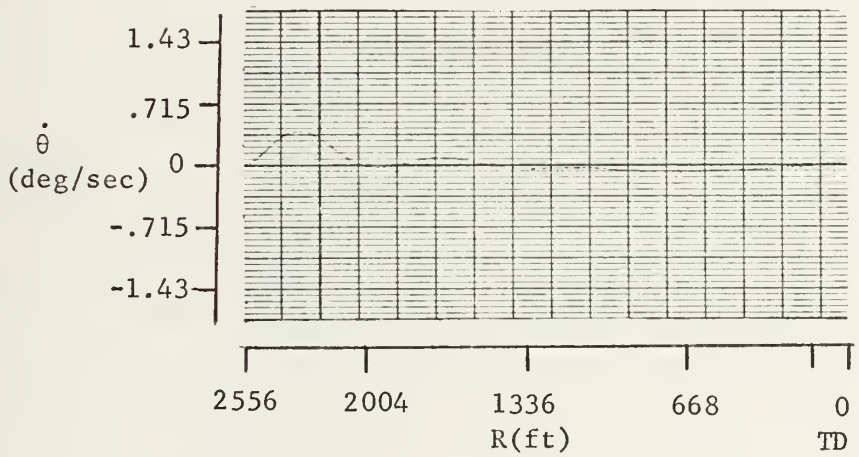


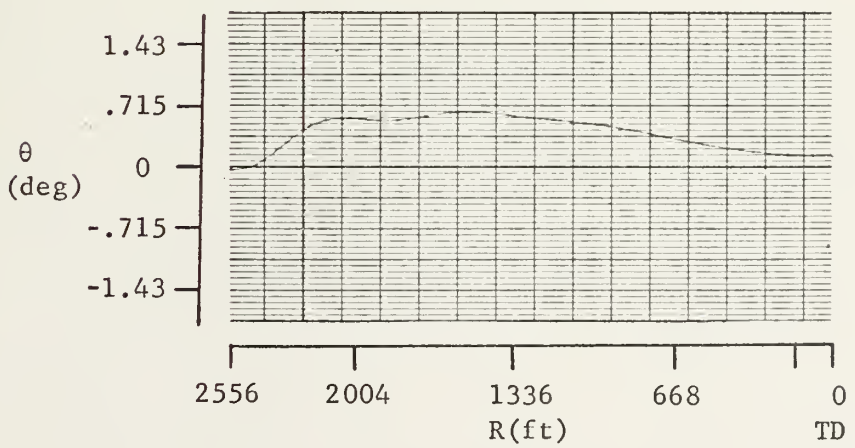


Figure 9 (continued)

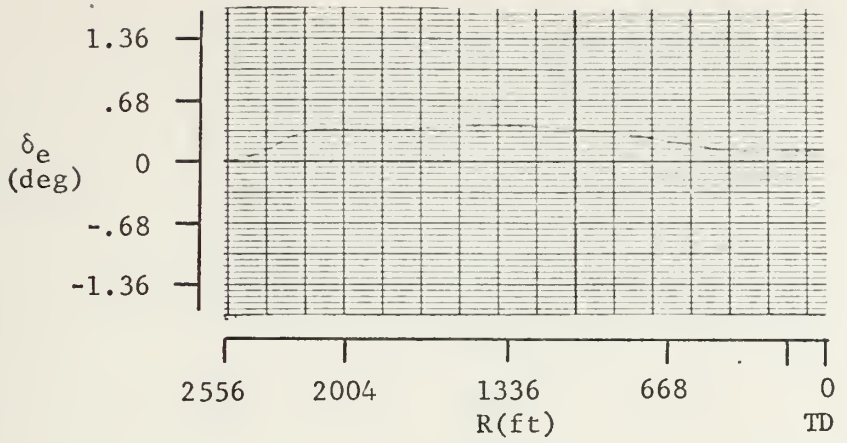


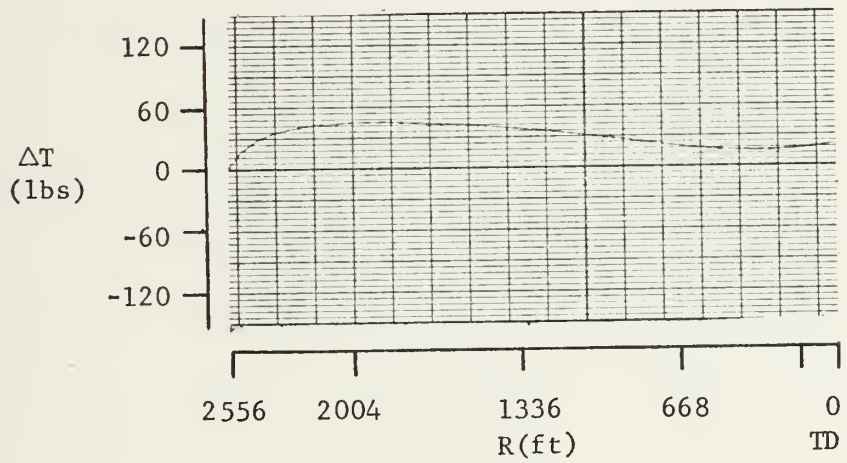


Figure 9 (continued)

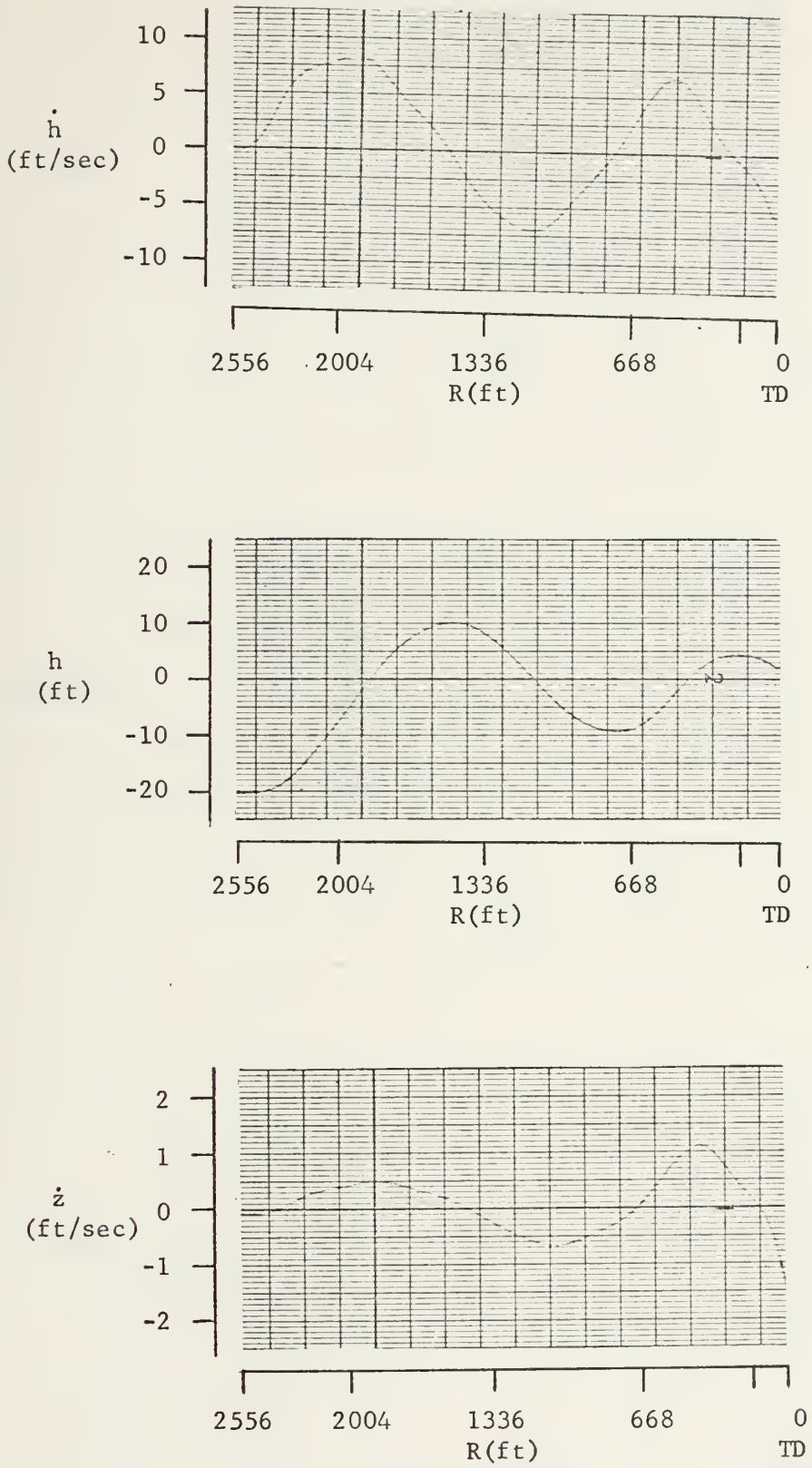


Figure 10. Approach recordings for $K_\theta$=-3.49rad/rad, $K_z$=0.072 rad/ft, $K_{\dot{z}}$=-0.167 rad/ft/sec. Initial condition: h=-20ft, z=-0.974ft. Note: Indifference Threshold Not In.

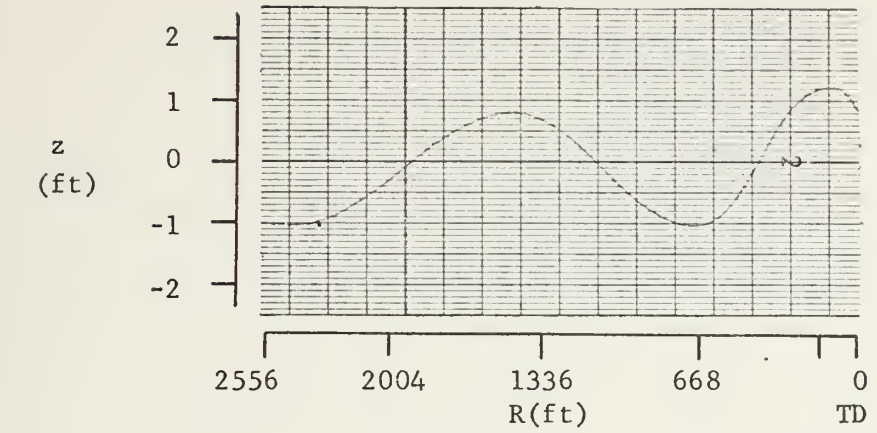


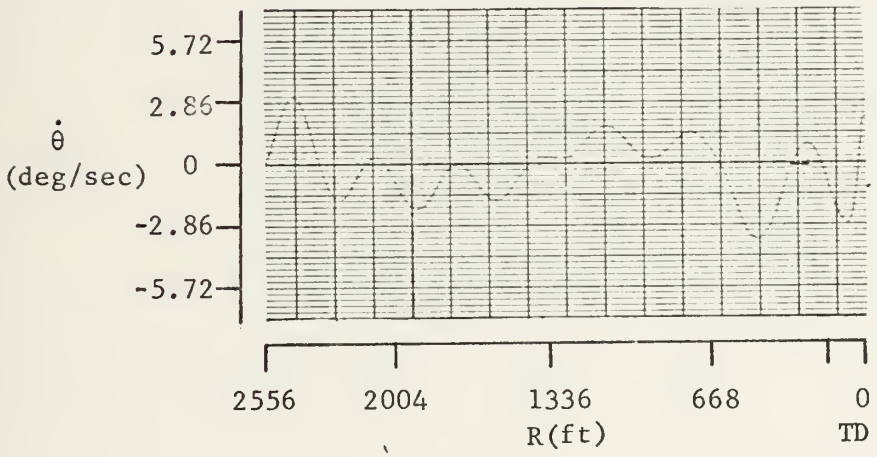


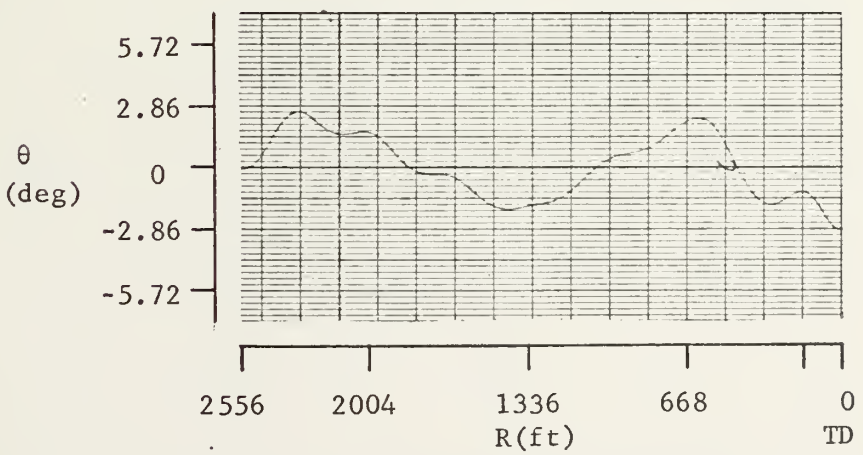


Figure 10(continued)

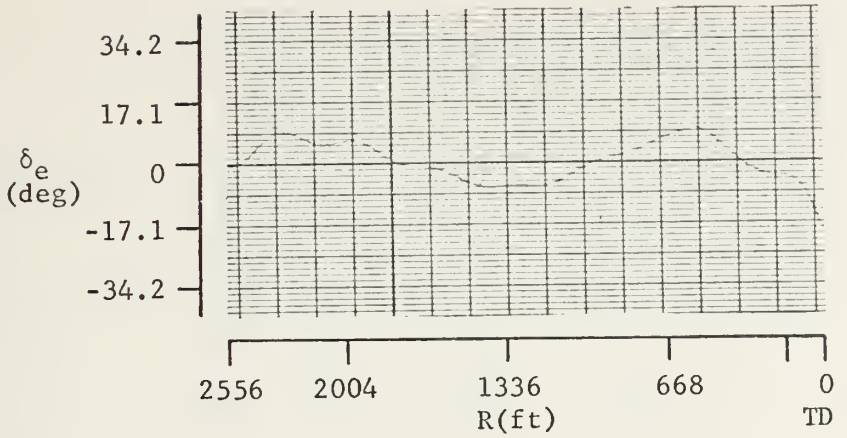


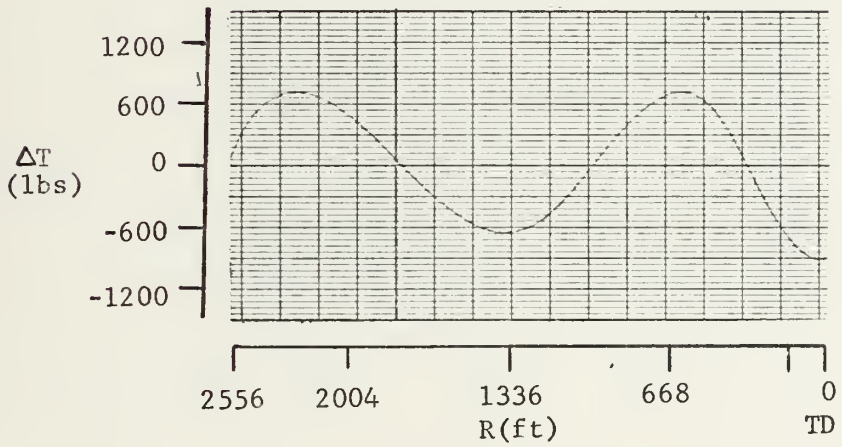


Figure 10 (continued)

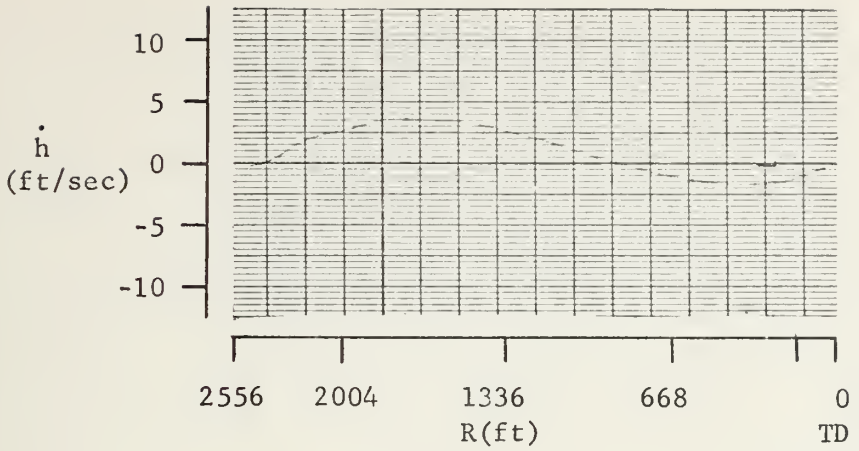


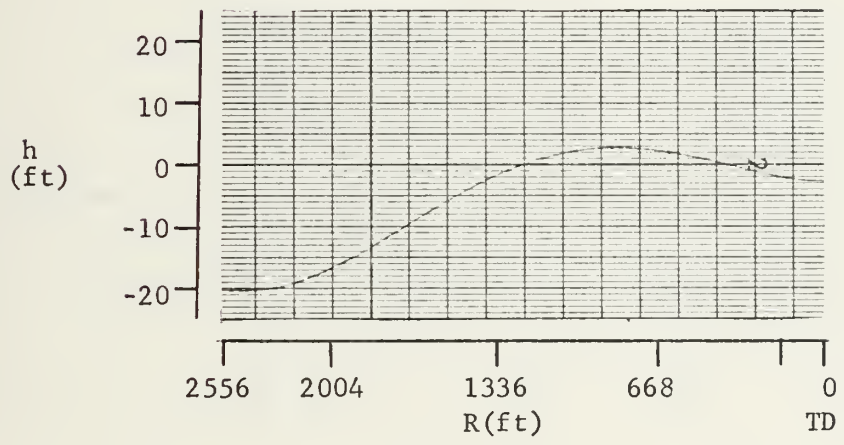


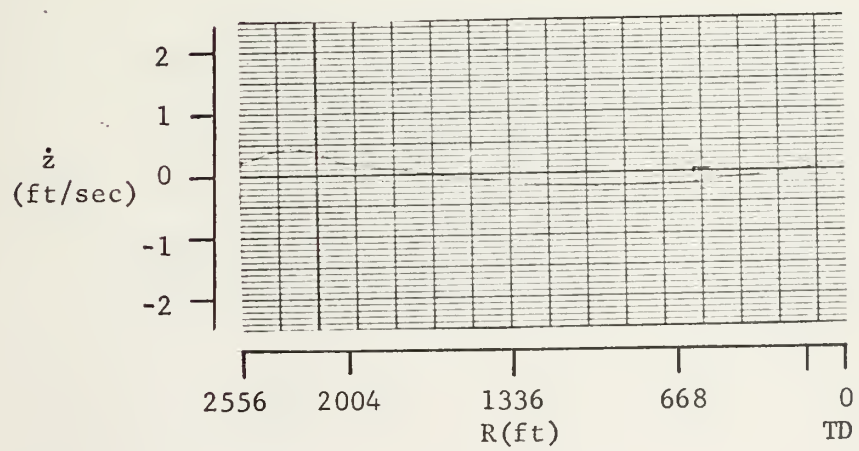


Figure 11. Approach recordings for $K_\theta$=-3.49 rad/rad, $K_{\dot{z}}$=0.0248 rad/ft, $K_z$=-0.167 rad/ft/sec. Initial condition: $\dot{h}$=-20ft, z=-0.974 ft. Note: Indifference Threshold Not In.

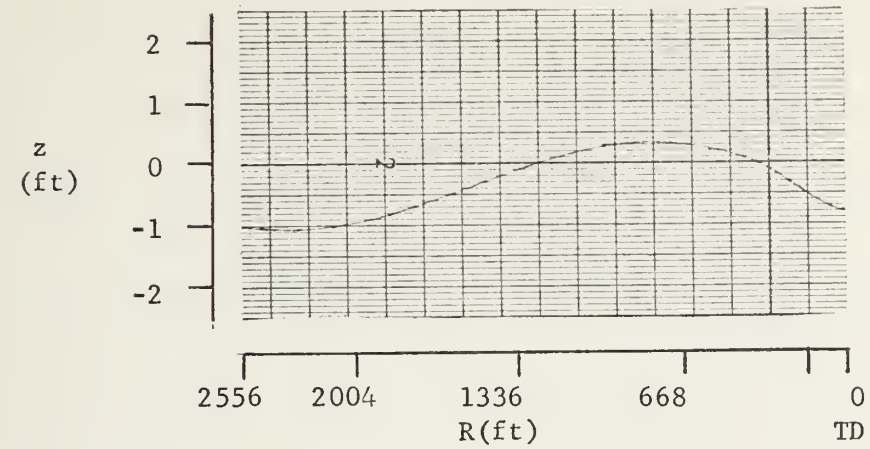


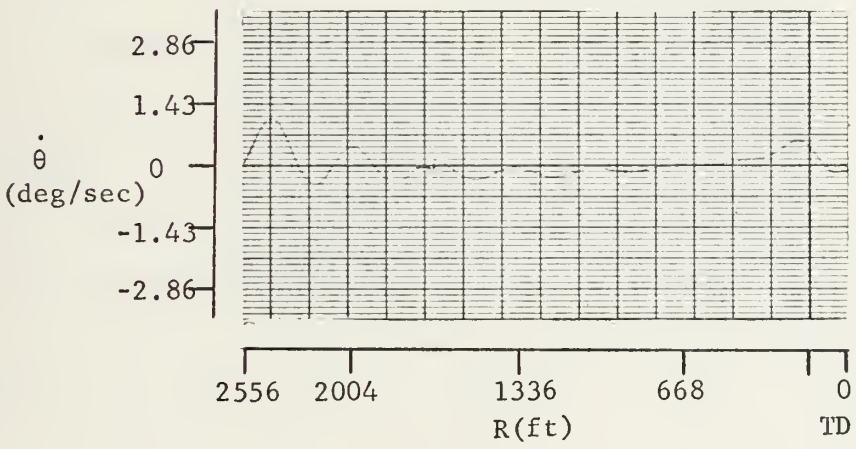


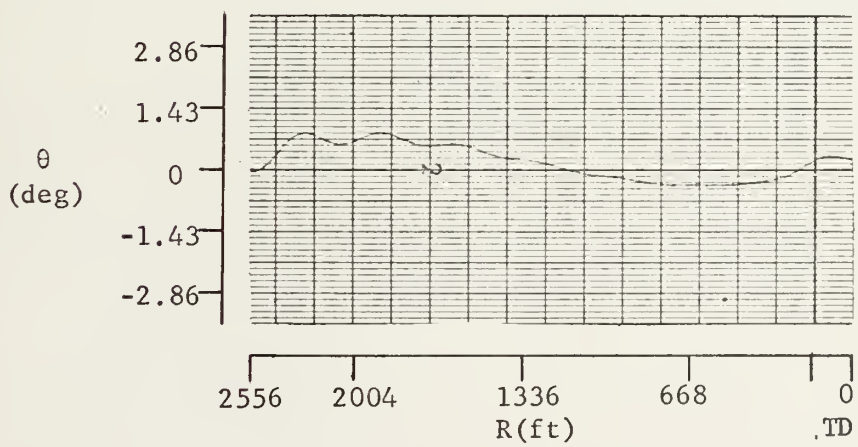


Figure 11 (Continued)

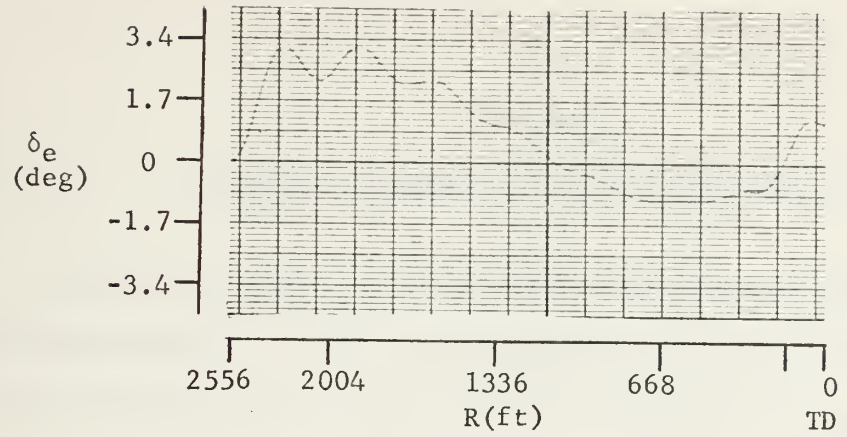


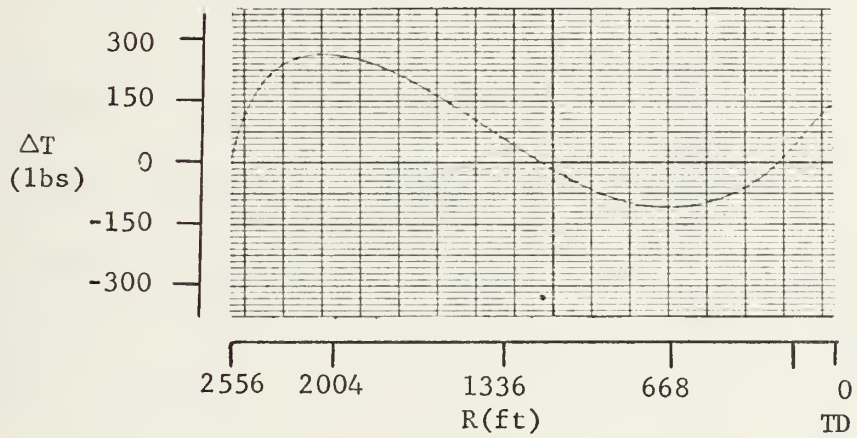


Figure 11 (continued)

## APPENDIX A

## EQUATIONS OF MOTION AND BASIC DATA FOR THE A7E

The A7E perturbational, linearized equations of motion are contained in this appendix. They are presented in matrix form as per Ref. [4]. The equations are about the stability axis and an operating point of trimmed level flight in a landing configuration. The basic data of the A7E is listed in Table A-1.

$$\begin{bmatrix} S-X_u^* & -X_w & g\cos\theta_o & 0 \\ -Z_u^* & (1-Z_{\dot{w}})S-Z_w & -U_oS+g\sin\theta_o & 0 \\ -M_u^* & M_{\dot{w}}S-M_w & S^2-M_qS & 0 \\ 0 & 1 & -U_o & 1 \end{bmatrix} \begin{bmatrix} u \\ w \\ \theta \\ \dot{h} \end{bmatrix}$$

$$\begin{bmatrix} X_{\delta_e} & X_{\Delta T} \\ Z_{\delta_e} & Z_{\Delta T} \\ M_{\delta_e} & M_{\Delta T} \end{bmatrix} \begin{bmatrix} \delta_e \\ \Delta T \end{bmatrix} \qquad \text{(A-1)}$$

TABLE A1

A7E GEOMETRY AND DIMENSIONAL AERODYNAMIC DERIVATIVES FOR A POWER APPROACH

| | | |
|---|---|---|
| $S = 375\ ft^2$ | $\bar{c} = 10.84$ ft | $Z_j = 0.271$ ft |
| $\alpha_{TL} = 10.73$ deg | W = 24,000 lbs | m = 746 slugs |
| C.G. at 28.6% MAC | $I_{yy} = 68{,}000\ slug\text{-}ft^2$ | $U_o = 218$ ft/sec |
| h = 0 ft | Mach = .1953 | |
| $\alpha_o = 12$ deg | $\rho = .002378\ slug/ft^3$ | |

DIMENSIONAL DERIVATIVES

| | | |
|---|---|---|
| $X_u^* = -0.054534$ | $X_w = 0.064327$ | $Z_u^* = 0.286953$ |
| $Z_{\dot{w}} = 0$ | $Z_w = -0.52871$ | $M_u^* = -0.000165$ |
| $M_{\dot{w}} = -0.000289$ | $M_w = -0.007964$ | $M_q = -0.372532$ |
| $X_{\delta_e} = 0.732836$ | $Z_{\delta_e} = -14.713536$ | $M_{\delta_e} = -2.188578$ |
| $X_{\Delta T} = 0.001317$ | $Z_{\Delta T} = -0.000250$ | $M_{\Delta T} = 0.000004$ |

## APPENDIX B

## POTENTIOMETER SETTINGS AND ANALOG COMPUTER DIAGRAM

The potentiometer settings and analog program are presented in Table B-1 below.

TABLE B-1

AMPLIFIER 01

pot 65 - 0.0395

pot 13 - 0.0044

pot 06 - 0.008

pot 05 - 0.0161

pot 21 - 0.0545

AMPLIFIER 31

pot 26 - 0.4800

pot 07 - 0.5234

pot 76 - 0.7811

pot 23 - 0.0006

pot 08 - 0.0328

pot 02 - 0.0328

AMPLIFIER 69

pot 18 - 0.100

pot 17 - 0.2439

AMPLIFIER 18

pot 19 - 0.100

AMPLIFIER 40

pot 34 - 0.0504

pot 04 - 0.0

pot 29 - 0.8051

AMPLIFIER 11

pot 66 - 0.0300

pot 25 - 0.3531

pot 33 - 0.1147

pot 32 - 0.5289

pot 31 - 0.0224

pot 15 - 0.218

AMPLIFIER 49

pot 12 - 0.545

pot 28 - 0.250

AMPLIFIER 50

pot 75 - 0.100

AMPLIFIER 48

pot 16 - 0.0100

AMPLIFIER 00

pot 00 - 0.0272

pot 11 - 0.0163

AMPLIFIER 20

pot 05 - 0.0904

AMPLIFIER 60

pot 24 - 0.0019

pot 14 - 0.0019

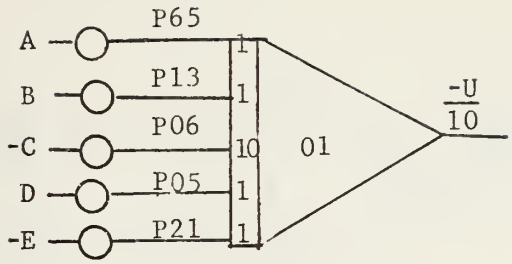


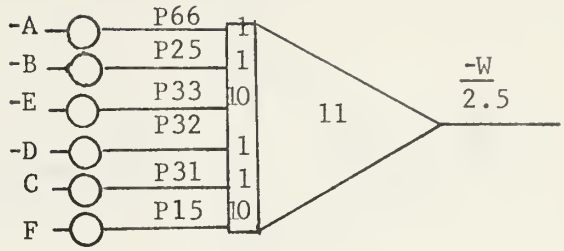


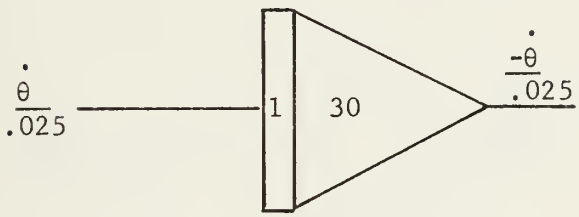


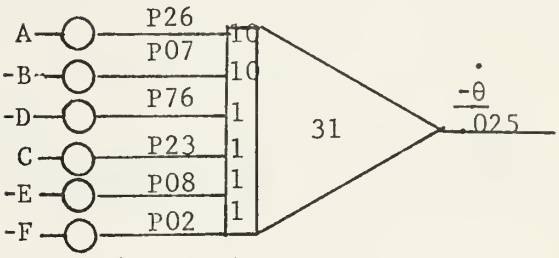


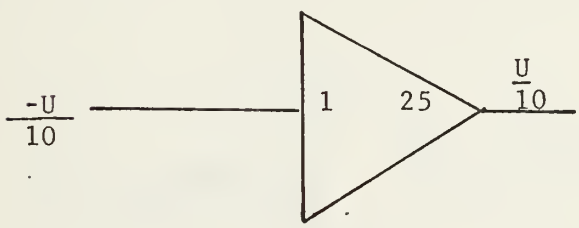


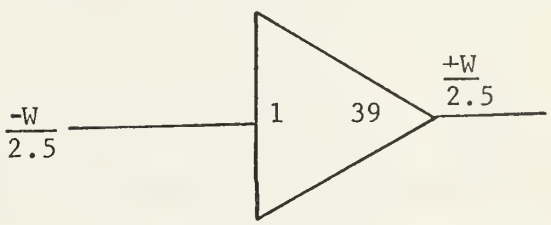


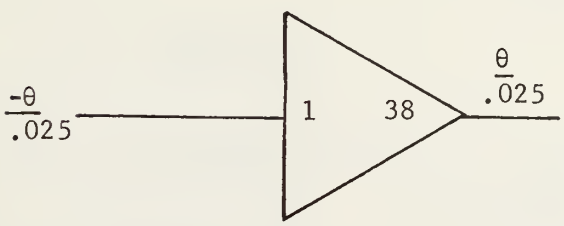


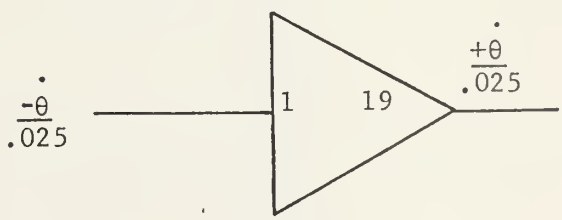


A = ΔT/300; B = $\delta_e$/0.06; C = θ/.025; D = W/2.5; E = U/10; F = $\dot{\theta}$/.025.

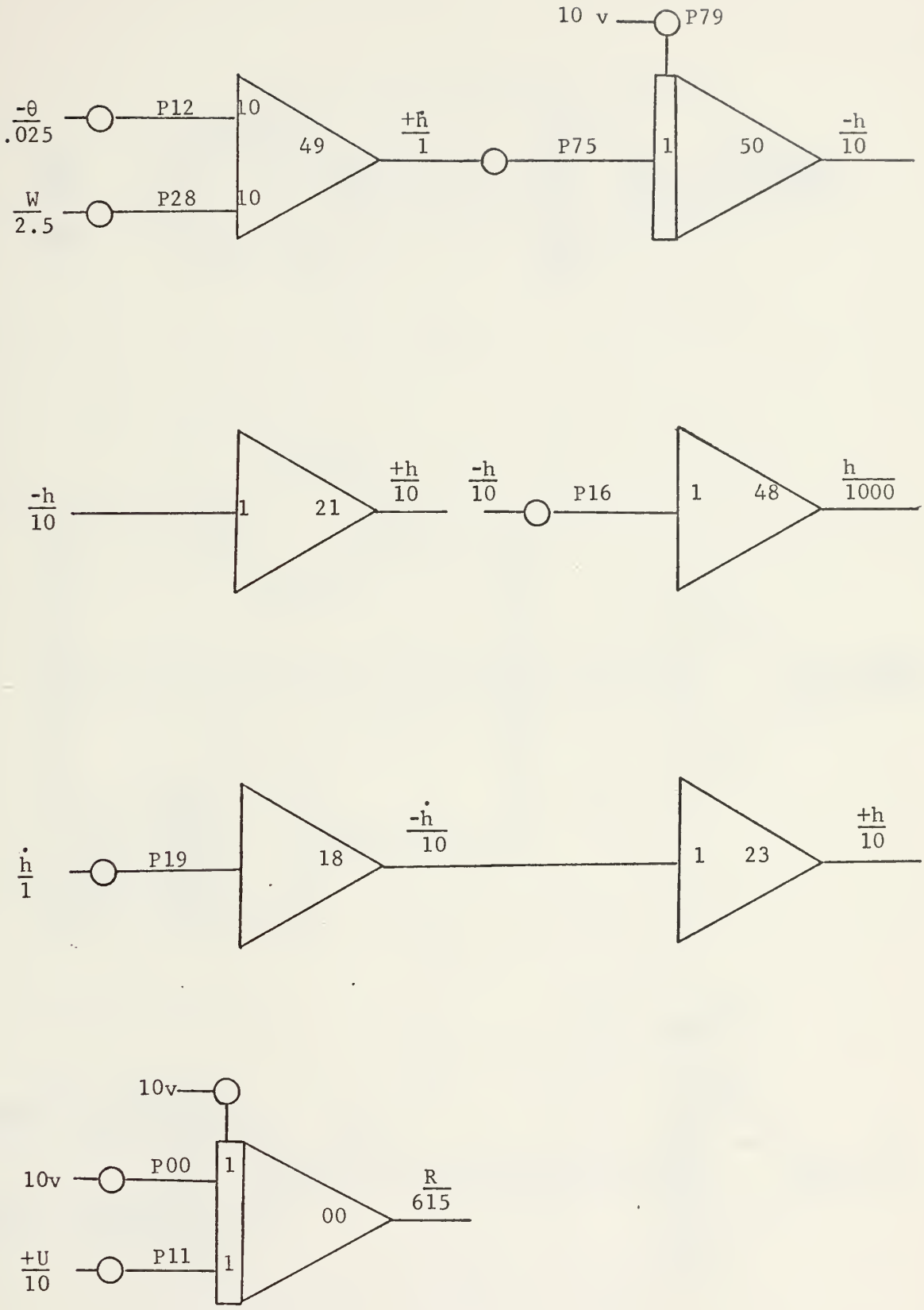
10 v
P79
-θ
.025
P12
10
49
+ḣ
1
P75
1
50
-h
10
W
2.5
P28
10
-h
10
1
21
+h
10
-h
10
P16
1
48
h
1000
ḣ
1
P19
18
-ḣ
10
1
23
+h
10
10v
10v
P00
1
00
R
615
+U
10
P11
1

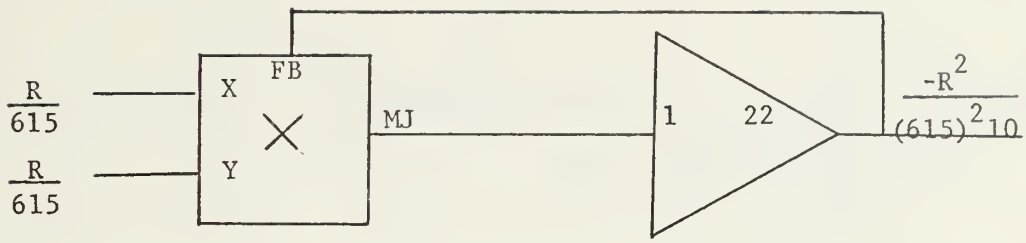
R/615
R/615
X
Y
FB
MJ
1
22
-R²/(615)²10

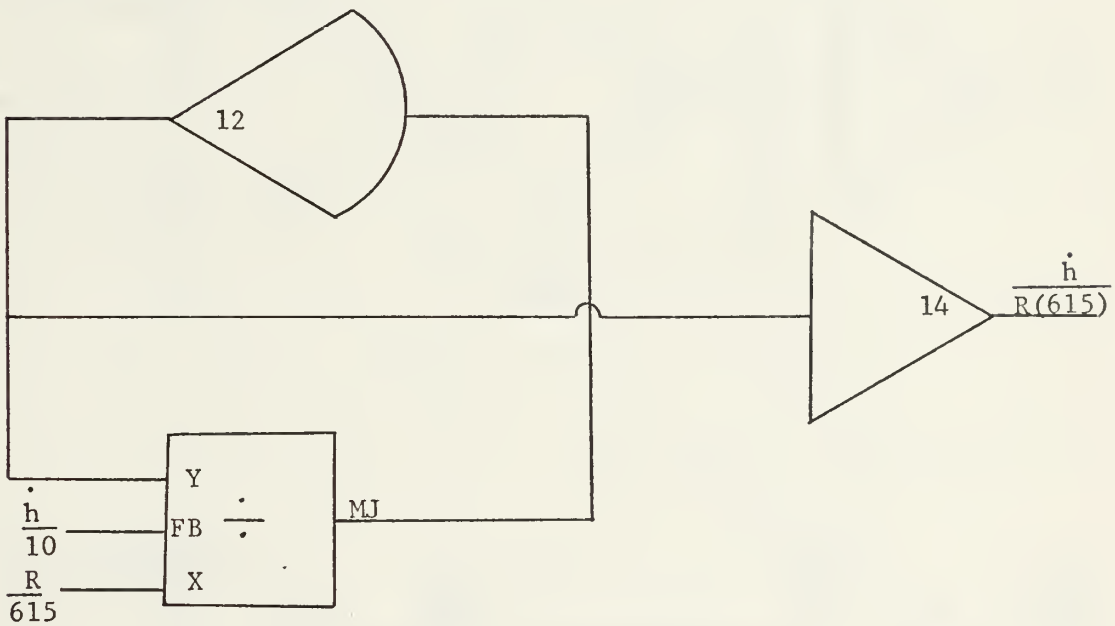
12
14
ḣ/R(615)
Y
FB
X
MJ
ḣ/10
R/615

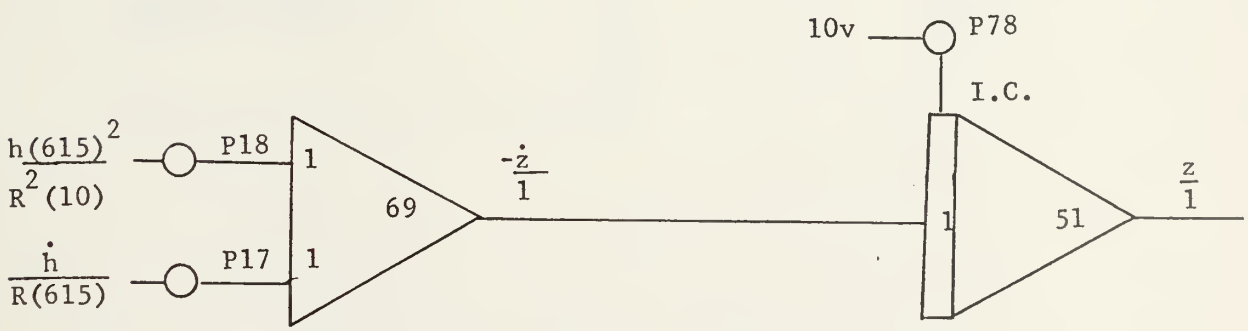
10v
P78
I.C.
h(615)²/R²(10)
P18
ḣ/R(615)
P17
1
1
69
-ż/1
1
51
ż/1

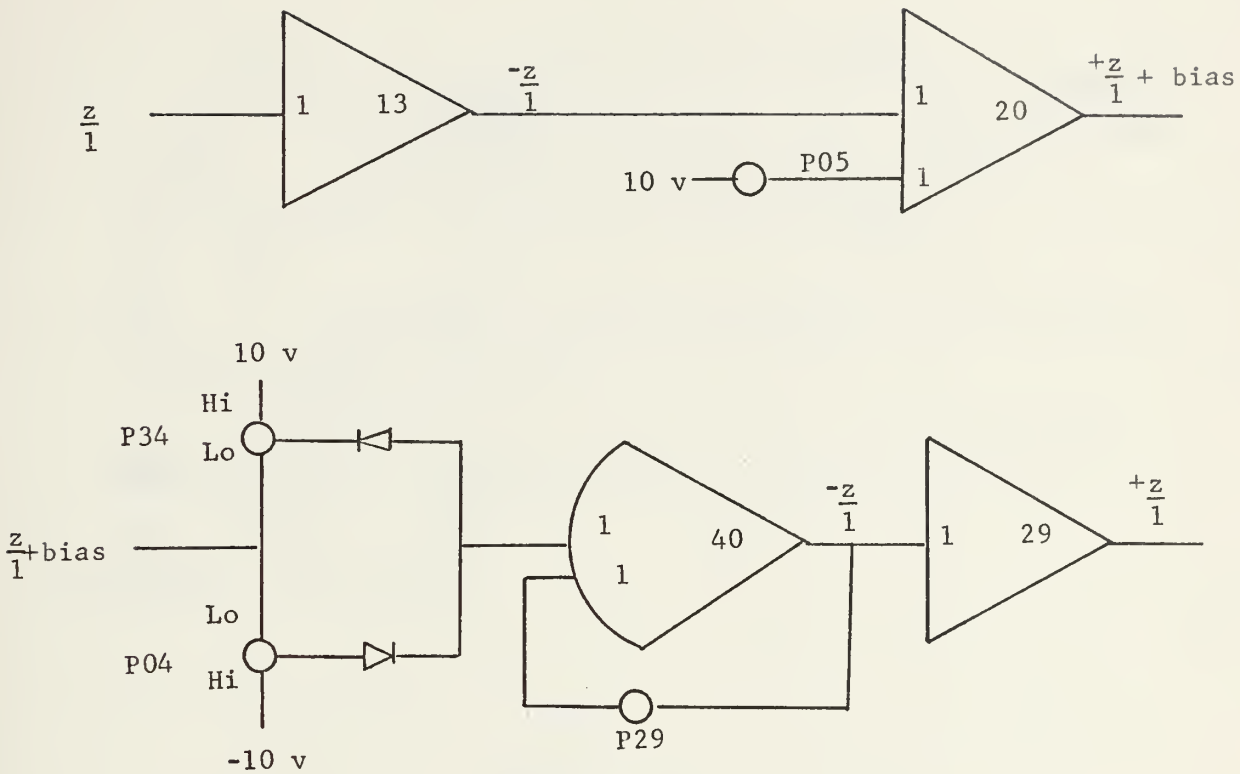
z/1
1
13
-z/1
1
20
+z/1 + bias
10 v
P05
1
10 v
Hi
P34
Lo
z/1+bias
Lo
P04
Hi
-10 v
1
40
1
-z/1
P29
1
29
+z/1

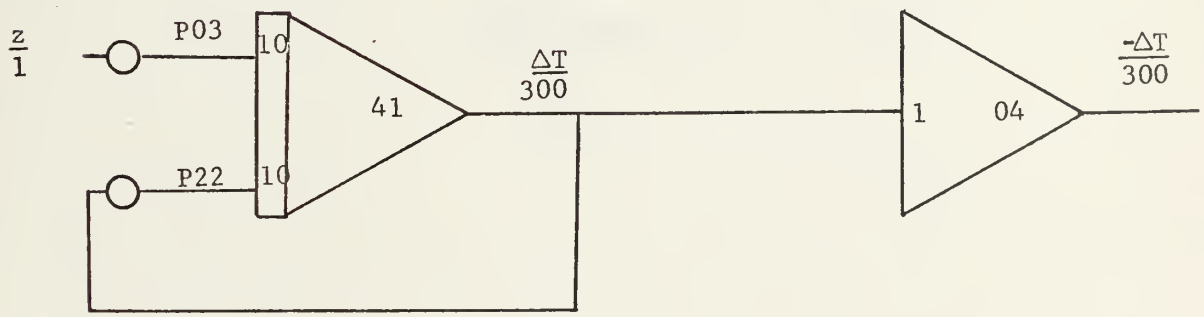
z/1
P03
10
P22
10
41
ΔT/300
1
04
-ΔT/300

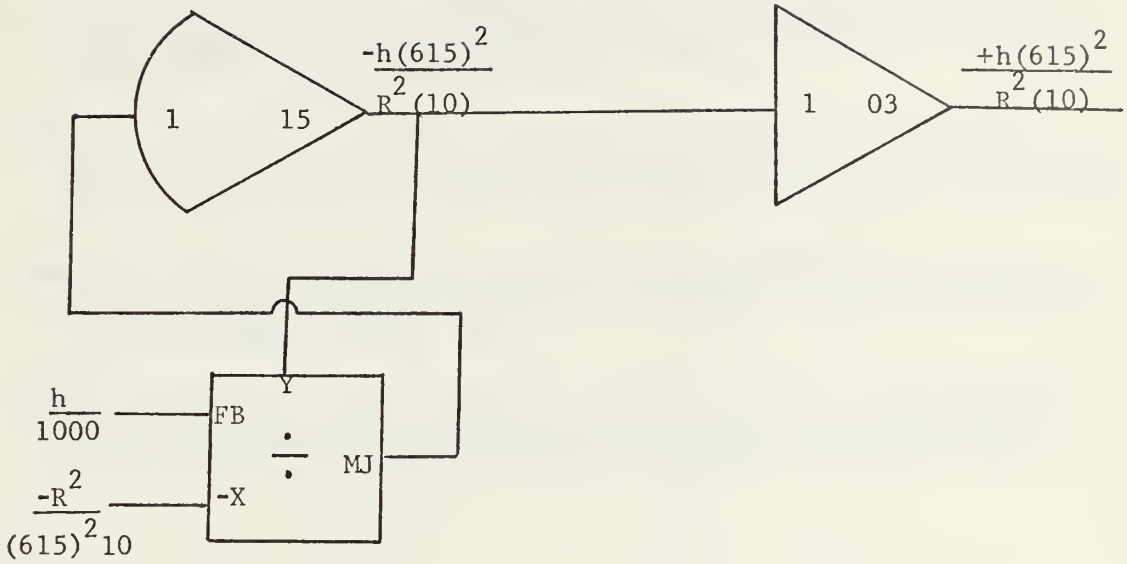
1 15
$\frac{-h(615)^2}{R^2(10)}$
1 03
$\frac{+h(615)^2}{R^2(10)}$
Y
$\frac{h}{1000}$
FB
MJ
$\frac{-R^2}{(615)^2 10}$
-X

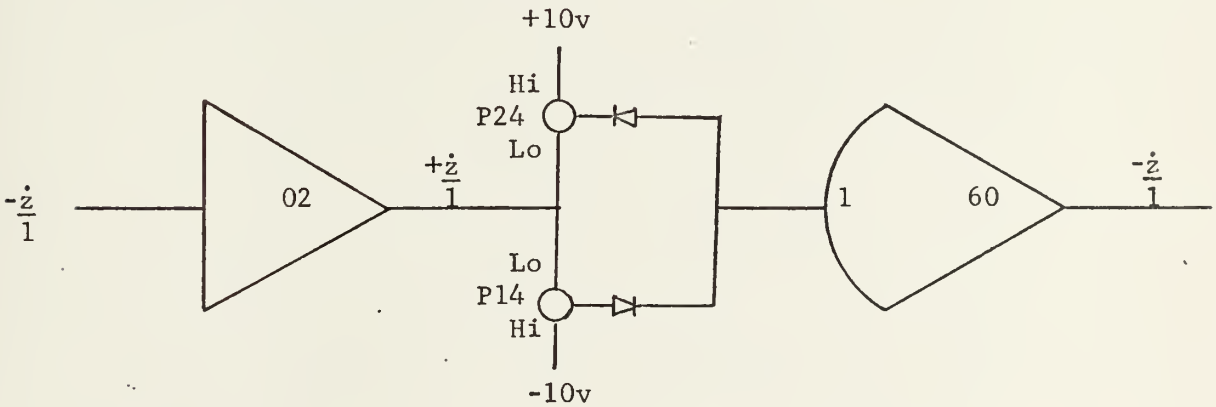
+10v
Hi
P24
Lo
$\frac{-\dot{z}}{1}$
02
$\frac{+\dot{z}}{1}$
1 60
$\frac{-\dot{z}}{1}$
Lo
P14
Hi
-10v

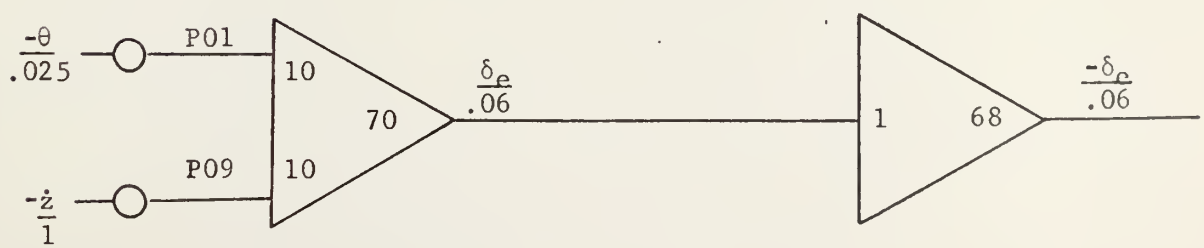
$\frac{-\theta}{.025}$
P01
10
70
$\frac{\delta_e}{.06}$
1 68
$\frac{-\delta_e}{.06}$
P09
10
$\frac{-\dot{z}}{1}$

## LIST OF REFERENCES


1. Systems Technology, Inc. Technical Report No. 137-1, An Analysis of Terminal Flight Path Control in Carrier Landing, by T.S. Durand and G.L. Teper, August 1964.

2. Naval Air Development Center, Air Vehicle Technology Department, Report in Preparation, Toward a Pilot Model for Carrier Approach, R.H. Smith and M.B. Reigle, March 1972.

3. Naval Air Development Center, Air Vehicle Technology Department, Report in Preparation, LSO/Pilot Interviews on Carrier Approach, by R.H. Smith, January 1971.

4. Systems Technology, Inc. Technical Report No. 197-1, An Analysis of Navy Approach Power Compensator Problems and Requirements, by S.J. Craig, R.F. Ringland and I.I.Ashkenas, March 1971.

INITIAL DISTRIBUTION LIST

| | | No. Copies |
|---|---|---|
| 1. | Defense Documentation Center<br>Cameron Station<br>Alexandria, Virginia 22314 | 2 |
| 2. | Library, Code 0212<br>Naval Postgraduate School<br>Monterey, California | 2 |
| 3. | Chairman, Department of Aeronautics<br>Naval Postgraduate School<br>Monterey, California 93940 | 1 |
| 4. | Asst. Professor M.H. Redlin<br>Department of Aeronautics<br>Naval Postgraduate School<br>Monterey, California 93940 | 1 |
| 5. | LT. Clark Albert Wilson<br>13051 Via Caballo Rojo<br>San Diego, California 92129 | 1 |

UNCLASSIFIED
Security Classification

DOCUMENT CONTROL DATA - R & D

(Security classification of title, body of abstract and indexing annotation must be entered when the overall report is classified)

1. ORIGINATING ACTIVITY (Corporate author)
Naval Postgraduate School
Monterey, California 93940

2a. REPORT SECURITY CLASSIFICATION
Unclassified

2b. GROUP

3 REPORT TITLE
The Simulation and Analysis of Carrier Landings Using a Nonlinear Pilot Model

4 DESCRIPTIVE NOTES (Type of report and, inclusive dates)
Master's Thesis; June 1973

5. AUTHOR(S) (First name, middle initial, last name)
Clark Albert Wilson

6. REPORT DATE
June 1973

7a. TOTAL NO. OF PAGES
61

7b. NO. OF REFS
4

8a. CONTRACT OR GRANT NO.

b. PROJECT NO.

c.

d.

9a. ORIGINATOR'S REPORT NUMBER(S)

9b. OTHER REPORT NO(S) (Any other numbers that may be assigned this report)

10. DISTRIBUTION STATEMENT
Approved for public release; distribution unlimited.

11. SUPPLEMENTARY NOTES

12. SPONSORING MILITARY ACTIVITY
Naval Postgraduate School
Monterey, California 93940

13. ABSTRACT

This report investigated the interaction of the pilot and the Fresnel lens optical landing system (FLOLS) with the aircraft system dynamics of a carrier landing and attempted to determine whether or not the dynamics of the FLOLS contributed to a nosedown command by the pilot when approaching touchdown.

With the assumption of a nonlinear pilot model, the entire system's equations of motion were programmed on an analog computer and time histories of approaches for various pilot gains were recorded and analyzed.

Results obtained showed that the stability of the entire system near touchdown was very sensitive to gains which the pilot adopted. Also, because of the lag in the FLOLS dynamics, the pilot would, for some pilot gains, input a definite nosedown command to counteract a rising meatball on the FLOLS display. The typical result of such a command is a hard landing or ramp strike.

DD FORM 1 NOV 68 1473 (PAGE 1)
S/N 0101-807-6811



UNCLASSIFIED
Security Classification

A-31408

| KEY WORDS | LINK A | | LINK B | | LINK C | |
|---|---|---|---|---|---|---|
| | ROLE | WT | ROLE | WT | ROLE | WT |
| Pilot Model | | | | | | |
| Carrier Landing | | | | | | |
| FLOLS | | | | | | |

145382
Thesis
W632 Wilson
c.1 The simulation and anal-
ysis of carrier landings
using a nonlinear pilot
model.